

Siting Requirements for Hydrogen Supplies Serving Fuel Cells in Non-combustible Enclosures

Research Project

Technical report



THE
FIRE PROTECTION
RESEARCH FOUNDATION

FIRE RESEARCH

THE FIRE PROTECTION
RESEARCH FOUNDATION

ONE BATTERYMARCH PARK
QUINCY, MASSACHUSETTS, U.S.A. 02169

E-MAIL: Foundation@NFPA.org

WEB: www.nfpa.org/Foundation

Siting Requirements for Hydrogen Supplies Serving Fuel Cells in Non-combustible Enclosures

Research Project

Technical report

Prepared by:

Jason Floyd, Ph.D.
Hughes Associates, Inc.



THE
FIRE PROTECTION
RESEARCH FOUNDATION

FIRE RESEARCH

THE FIRE PROTECTION
RESEARCH FOUNDATION

ONE BATTERYMARCH PARK
QUINCY, MASSACHUSETTS, U.S.A. 02169
E-MAIL: Foundation@NFPA.org
WEB: www.nfpa.org/Foundation

© Copyright The Fire Protection Research Foundation
November 2006

Foreword

Advancements in fuel cell technologies have made hydrogen fueled backup power systems competitive with traditional battery or combustion engine driven generating systems. For larger applications, these systems can require on-site storage of a number of hydrogen storage cylinders. These are typically stored in non-combustible cabinets. Currently, the NFPA 55 document for hydrogen storage does not explicitly address siting requirements for hydrogen cylinders stored in this manner. The primary goal of this project was to develop technical information to support the creation of new NFPA 55 requirements for storing less than 3500 ft³ of hydrogen in metal storage cabinets.

This project focused on determining the hazard posed by a variety of scenarios involving the release of hydrogen from a storage enclosure and associated equipment. Results of the hazard determination were used to evaluate siting requirements for a variety of threats or targets.

The Research Foundation expresses gratitude to the report authors at Hughes Associates, Inc.; Project Technical Panelists William Barlen, Larry Fluer, Charles Henrici, Carl Rivkin, Michael St. Clair, and Michael Swain; and project sponsors Idatech LLC, Plug Power Inc., Relion, Inc., US Fuel Cell Council, US Department of Energy, and UTC Fuel Cells.

The content, opinions and conclusions contained in this report are solely those of the authors.

Siting Requirements for Hydrogen Supplies Serving Fuel Cells in Non-combustible Enclosures

Research Project

Technical Panel

William Barlen, Barlen and Associates, Inc.

Larry Fluer, Fluer, Inc.

Charles Henrici, Elk Grove Village, IL

Carl Rivkin, NFPA

Michael St. Clair, Ohio State University

Michael Swain, University of Miami

Sponsors

Idatech LLC

Plug Power Inc.

Relion, Inc.

US Fuel Cell Council

US Department of Energy

UTC Fuel Cells

**SITING REQUIREMENTS FOR HYDROGEN SUPPLIES
SERVING FUEL CELLS IN NON-COMBUSTIBLE
ENCLOSURES**

Prepared for:

Kathleen Almand
The Fire Protection Research Foundation
1 Batterymarch Park
Quincy, MA 02169

Prepared by:

Jason Floyd, Ph.D.



HUGHES ASSOCIATES, INC.
FIRE SCIENCE & ENGINEERING

3610 Commerce Drive, Suite 817
Baltimore, MD 21227-1652
410-737-8677 Fax 410-737-8688

HAI Project # 3250-000

November 30, 2006

TABLE OF CONTENTS

TABLE OF CONTENTS.....	ii
LIST OF TABLES	iii
LIST OF FIGURES	iv
1.0 INTRODUCTION	1
2.0 STUDY INPUT DATA	2
2.1 Generic Enclosure	2
2.2 Study Scenarios.....	3
3.0 DISCUSSION OF RELATED RESEARCH.....	6
4.0 FIRE DYNAMICS SIMULATOR	7
4.1 Overview of FDS	7
4.2 Discussion of Related Validation.....	8
5.0 DESCRIPTION OF FDS SIMULATIONS	12
5.1 Enclosure Releases.....	12
5.2 Emergency Vent Releases.....	16
5.3 External Piping Releases.....	18
6.0 DISCUSSION OF DATA ANALYSIS	19
6.1 FDS Output Postprocessing	19
6.2 Explosion Hazard.....	19
6.3 Burn/Deflagration Hazard.....	20
7.0 RESULTS	21
7.1 Summary of Computations	21
7.2 Explosion	25
7.3 Burn/Deflagration Results	28
7.4 Alternate Enclosure Scenario.....	33
8.0 CONCLUSIONS.....	33
9.0 ACKNOWLEDGEMENTS.....	35
10.0 REFERENCES	36

LIST OF TABLES

Table 1: Test Matrix for Internal Release	4
Table 2: Test Matrix for Emergency Vent Release	5
Table 3: Test Matrix for Release from External Piping.....	6
Table 4: FDS Predictions of 20 SCFM Hydrogen Jet vs. Measured Data.....	11
Table 5: Explosion Results Matrix for Internal Release	27
Table 6: Explosion Results Matrix for Emergency Vent Release	28
Table 7: Explosion Results Matrix for Release from External Piping.....	28
Table 8: Plume Extents Results Matrix for Internal Release.....	29
Table 9: Plume Extents Results Matrix for Emergency Vent Release	30
Table 10: Plume Extents Results Matrix for Release from External Piping.....	30
Table 11: Radiative Results Matrix for Internal Release.....	31
Table 12: Radiative Results Matrix for Emergency Vent Release	32
Table 13: Radiative Results Matrix for Release from External Piping	32
Table 14: Radiative Results Matrix for Quasi-steady Burning at Leak Source.....	33
Table 15: Results of Lower Pressure and Alternate Gas Simulations	33
Table 16: Effect Distances for Various Targets.....	34

LIST OF FIGURES

Figure 1: Generic Hydrogen Storage Enclosure	2
Figure 2: Three Leak Types Analyzed.....	3
Figure 3: FDS vs. Integral Jet Model and Chen-Rodi Correlations.....	9
Figure 4: FDS vs. Data for a 7.3 cm Diameter 0.45 m/s Helium Plume	10
Figure 5: FDS Predictions of a 566 L/min SCFM Hydrogen Jet through a 9.45 mm Orifice.....	11
Figure 6: Time Dependent Leak Rate for a Single 450 bar Bottle Emptying Through a 0.00635 m Diameter Leak (PRD Failure).....	13
Figure 7: Time Dependent Leak Rate for Three 450 bar Bottles Emptying Through a 0.00127 m Diameter Leak (Internal Piping Failure).....	14
Figure 8: FDS Input Geometry for Internal Leaks.....	15
Figure 9: Emergency Vent Pipe Exit	16
Figure 10: PRD Failure, 0.4 Vent Size, Perpendicular 2.2 m/s Wind	21
Figure 11: Internal Piping Leak, Face Vent.....	22
Figure 12: Emergency Vent of Regulator Failure, 2.2 m/s Wind.....	22
Figure 13: Emergency Vent of Pinhole Leak, 2.2 m/s Wind.....	23
Figure 14: Ground Level 150 psig Pipe Leak, 2.2 m/s Wind	23
Figure 15: Ground Level 85 psig Pipe Leak, 2.2 m/s Wind	24
Figure 16: Scatter Plot of the Hydrogen Mass between the LFL and UFL and the LEL and the UEL for the Ridge Vent PRD Failure Scenarios (-1 m/s Wind = Sinusoidal Wind Speed).....	24
Figure 17: Scatter Plot of the Hydrogen Mass between the LFL and UFL and the LEL and the UEL for the for the External Pipe Leak Scenarios (-1 m/s Wind = Sinusoidal Wind Speed).....	25

Siting Requirements For Hydrogen Supplies Serving Fuel Cells In Non-Combustible Enclosures

1.0 INTRODUCTION

Advancements in fuel cell technologies have made hydrogen fueled backup power systems competitive with traditional battery or combustion engine driven generating systems. For larger applications, these systems can require on-site storage of a number of hydrogen storage cylinders. These are typically stored in non-combustible cabinets. Currently, the NFPA 55 document for hydrogen storage does not explicitly address siting requirements for hydrogen cylinders stored in this manner. The primary goal of this project was to develop technical information to support the creation of new NFPA 55 requirements for storing less than 3500 ft³ of hydrogen in metal storage cabinets.

This project focused on determining the hazard posed by a variety of scenarios involving the release of hydrogen from a storage enclosure and associated equipment. A generic storage enclosure was defined by an industry panel serving as oversight for this project. Additionally, the release scenarios were also defined in advance. There were three groups of scenarios: releases directly from the bottles within the enclosure, releases through an emergency vent, and releases from piping outside the enclosure. Each group of scenarios examined a range of release rates and ambient wind conditions.

All the releases were modeled with Fire Dynamics Simulator (FDS), a low-Mach number, large eddy simulation (LES), computational fluid dynamics code (CFD) written by the Building and Fire Research Laboratory (BFRL) at the National Institute of Standards and Technology (NIST). The simulations were used to define the volume and mass of hydrogen within the flammable and explosive limits for each scenario. This data was then used to determine the potential hazard if ignition occurred.

Results of the hazard determination were used to determine siting requirements for the following types of outdoor threats or targets:

1. Public sidewalks and parked vehicles
2. Ignition sources
3. Lot line
4. Buildings – combustible or non combustible walls; wall openings (including doors, windows and other openings) located either more or less than 25 feet above grade; air compressor intakes or inlets to ventilating or air-conditioning equipment.
5. Above ground flammable gas storage other than hydrogen above or below ground.

It is noted that this project did not perform an assessment of the risk posed by each hazard. Neither the probability of the release scenarios occurring nor the probability of the consequence occurring (i.e. ignition of a deflagration or detonation) was considered.

2.0 STUDY INPUT DATA

2.1 Generic Enclosure

A generic enclosure was defined by an industry panel. The enclosure was defined as a rectangular parallelepiped capable of holding twelve compressed gas cylinders of hydrogen with a cross section of 48" (1.22 m) x 36" (0.91 m) and a height of 65" (1.65 m). A gas cylinder, including the valve stem, has nominal dimensions of 9" (0.23 m) x 60" (1.52 m). The free air volume of the enclosure is approximately 1 m³. The enclosure will contain either a vent on a face of the enclosure or a vent on the ridgeline of the enclosure. The ridge vent is open around its sides and the total area of the vent is defined as a fraction of the enclosure floor area. The face vent consisted of a rectangular opening on one of the small faces of the enclosure with its top edge at 1.5 m. A cut-away view rendering of the enclosure with a ridge line vent is shown in Figure 1 below. In addition to the bottles the enclosure will contain piping, regulator valves, and an emergency vent system. Details of additional equipment in the enclosure were not provided; however, they are not necessary for the analysis in this report.

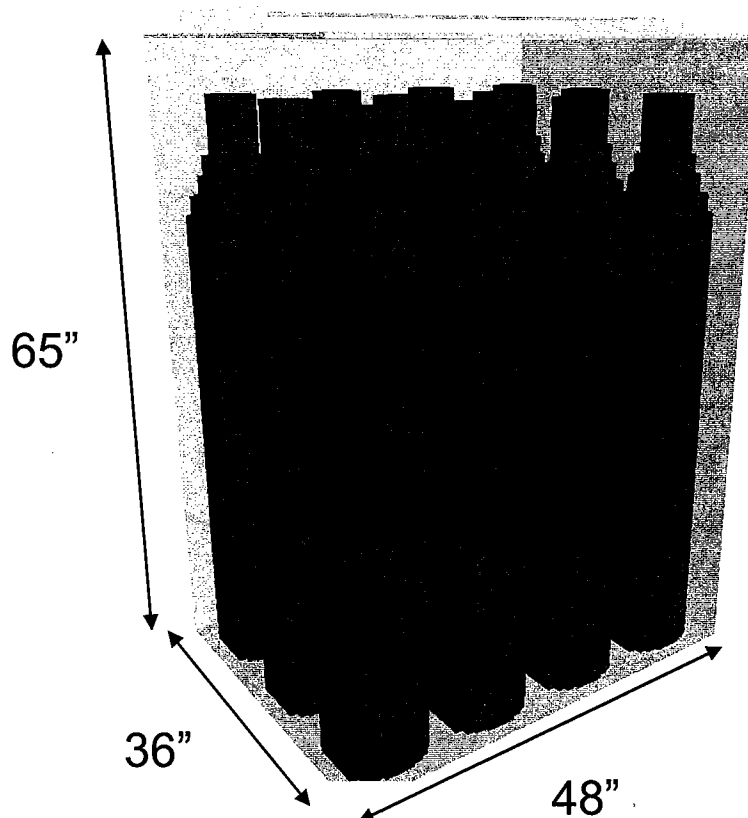


Figure 1: Generic Hydrogen Storage Enclosure

2.2 Study Scenarios

Three groups of release scenarios were performed in this study. The scenarios and permutations of the scenarios were fully defined by an industry panel. The scenario definitions are discussed in detail below. The first set of scenarios examined hydrogen releases internal to the enclosure where the hydrogen exited through the roof vent of the enclosure. The second set of scenarios examined pressure relief through the enclosure's emergency vent. The final set of scenarios examined leaks in piping that is external to the enclosure. Figure 2 below depicts the three leak types.

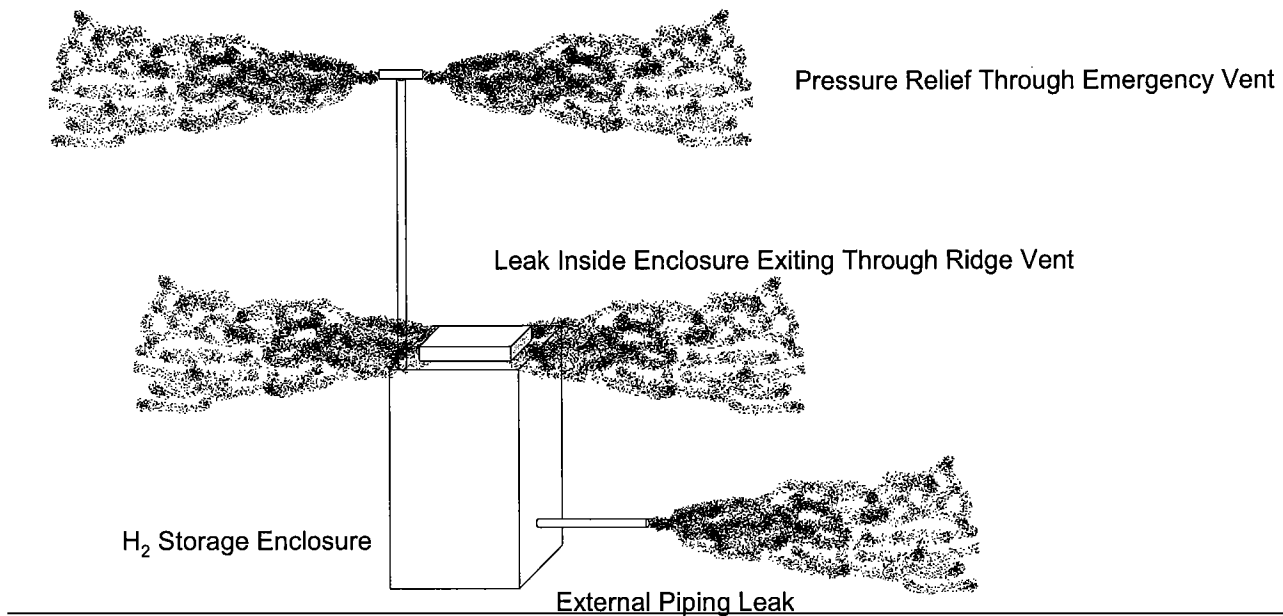


Figure 2: Three Leak Types Analyzed

Two internal leaks were analyzed. The first internal leak assumed that a pressure relief device (PRD) on a single bottle (0.00635 m hole diameter) failed. This leak will be referred to as the PRD failure scenario. The second internal leak assumed that a leak (0.00127 m hole diameter) occurred on piping that was connected to three bottles. This leak will be referred to as the internal piping scenario. Both of these scenarios assume the leak pressure is 450 bar (6530 psi). Table 1 below provides a summary of these scenarios and their permutations as defined by the panel.

Table 1: Test Matrix for Internal Release

Inventory (bottles)	Wind Speed (m/s)	Vent Location	Vent Area (m ² vent/m ² floor area)	Wind Direction with Respect to Vent	Wind Variation
1 (PRD)	2.2	Ridge-line	0.10	Parallel	None
			0.10	Perpendicular	
			0.22	Parallel	
			0.22	Perpendicular	
			0.40	Parallel	
			0.40	Perpendicular	
	4.5		0.10	Parallel	
			0.10	Perpendicular	
			0.22	Parallel	
			0.22	Perpendicular	
			0.40	Parallel	
			0.40	Perpendicular	
	9.0		0.10	Parallel	
			0.10	Perpendicular	
			0.22	Parallel	
0.22		Perpendicular			
0.40		Parallel			
0.40		Perpendicular			
3 (piping)	2.2	Ridge-line	0.10	Parallel	None
			0.10	Perpendicular	
			0.22	Parallel	
			0.22	Perpendicular	
			0.40	Parallel	
			0.40	Perpendicular	
	4.5		0.10	Parallel	
			0.10	Perpendicular	
			0.22	Parallel	
			0.22	Perpendicular	
			0.40	Parallel	
			0.40	Perpendicular	
	9.0		0.10	Parallel	
			0.10	Perpendicular	
			0.22	Parallel	
0.22		Perpendicular			
0.40		Parallel			
0.40		Perpendicular			
1 (PRD)	4.5	Face	0.10	Parallel	
3 (piping)				Perpendicular	
				Parallel	
				Perpendicular	
1 (PRD)	4.5	Ridge-line	0.22	Parallel	Sinusoidal 0.3 Hz ± 2 m/s
3 (piping)				Perpendicular	
				Parallel	
				Perpendicular	

The second set of scenarios examined releases of hydrogen through the emergency vent. Two leak rates of 70.8 m³/min (regulator failure scenario) and 1.4 m³/min (pinhole leak scenario) were examined. Table 2 below provides a summary of these release scenarios and their permutations as defined by the panel. Two vent heights were specified: 3 m and 6 m. Only the 3 m cases were simulated as results from the 3 m cases indicate that the 6 m results can be obtained by vertical translation of the 3 m results (i.e. the effect of the ground on a 3 m release is not significant)

Table 2: Test Matrix for Emergency Vent Release

Failure Mode	Leak Rate (m ³ /min)	Wind Speed (m/s)	Vent Height (m)	Wind Variation
Regulator	70.8	2.2	3	None
			6	
		4.5	3	
			6	
		9.0	3	
			6	
Pinhole	1.4	2.2	3	
			6	
		4.5	3	
			6	
		9.0	3	
			6	
Regulator	70.8	4.5	3	Sinusoidal 0.3 Hz ± 2 m/s
Pinhole	1.4			

*Note: Based on 3 m results, 6 m vent height scenarios were not run

It is noted that regulator failure seems to be a very large flow rate in comparison to typical fuel cell systems used for backup power. Assuming a 50 % efficient fuel cell, 70.8 m³/min corresponds to 7 MW of power generation. At that flow rate, the twelve bottles in the enclosure would empty in 5 minutes. Assuming a 4 hour backup capability with a regulator sized to twice the required flow rate, a regulator failure of only 3.4 m³/min is obtained (i.e. somewhat larger than the postulated pinhole leak).

The final set of scenarios examined releases from piping outside the enclosure at two leak rates of either 4.2 kg/hr (85 psig leak scenario) or 6.9 kg/hr (150 psig leak scenario). Table 3 below provides a summary of these release scenarios and their permutations as defined by the panel.

Table 3: Test Matrix for Release from External Piping

Failure Mode	Leak Rate (kg/hr)	Wind Speed (m/s)	Leak Height (m)	Wind Variation
85 psig leak	4.2	2.2	0	None
			1	
		4.5	0	
			1	
		9.0	0	
			1	
150 psig leak	6.9	2.2	0	
			1	
		4.5	0	
			1	
		9.0	0	
			1	
85 psig leak	4.2	4.5	0	Sinusoidal 0.3 Hz ± 2 m/s
150 psig leak	6.9			

3.0 DISCUSSION OF RELATED RESEARCH

Matthijsen and Kooi performed a risk analysis study of hydrogen filling stations [16] for the Dutch Ministry of Housing, Spatial Planning, and the Environment. This study evaluated the separation distances from a hydrogen filling station required to have an individual risk (IR) less than a 10^{-6} death/per person-year and to result in less than 1 % fatality rate in the event of an accident (using a 9.8 kW/m^2 heat flux criteria). For a medium size, 350 bar (5100 psig), filling station these distances are respectively 11 m and 29 m. The fatality rate distance is larger as it does not include the probability of occurrence. A 700 bar (10300 psig) station has an acceptable IR separation distance of 15 m. The study evaluated the effect distance as a function of wind speed between 1.5 and 9 m/s and determined that the effect distance for a jet fire varied between 17 m and 12.5 m respectively.

Brown, et. al [17] performed a risk analysis of a large hydrogen storage tank for the State Environment Agency of Sao Paulo State, Brazil. Using a method similar to that discussed above, the IR contour (10^{-6} death/yr) for the storage tank ranged from 75 m to 125 from the storage tank. While the volume of the storage tank is not provided in the paper, given that it is being used as chemical feedstock, it is likely larger than the 3500 ft^3 or less of hydrogen storage being considered in this project.

Xu, et al. [18] performed numerical studies of a vertical, sonic hydrogen jet using a compressible flow, commercial CFD code (CFX). These studies indicated that volume concentrations of 20 % remained at the centerline 300 diameters from the jet source. For the emergency vent release scenarios described in Section 2.0 this would be a distance of up to 7.6 m from the vent.

Shivrvill, et al [19] performed experiments of ignited and unignited hydrogen jets into still (< 2 m/s wind) air. One experiment released 25 bar (350 psig) hydrogen through a 12 mm orifice. This is a similar release to the 6.9 kg/hr pipe leak which is 10 bar through a 2 mm leak. Concentrations of 4 % hydrogen were measured 10 m downstream of the leak.

Takeno, et. al [20] performed experiments that released a 250 L inventory of hydrogen at 395 bar (5800 psi) through a variety of orifices. A downstream igniter was used to ignite the gas cloud and pressure measurements were made of the resulting pressure wave. For flow rates consistent with the PRD failure scenario pressures in excess of 1 psi were measured at radial distances of 10 m from the leak source.

Note that with the exception of the work by Swain, et. al [12], the commercial CFD codes were likely run in a steady-state mode. Additionally it is likely that all methods used a k- ϵ like turbulence model. Steady-state computations by their nature will lessen the extent of the flammable volume as they will not account for the impact of puffing behavior. k- ϵ models, even in time dependent mode, will also act to smooth the effects of puffing behaviors over relatively large time scales. LES models also result in averaging, however, over smaller length and timescales than typical for k- ϵ models.

4.0 FIRE DYNAMICS SIMULATOR

4.1 Overview of FDS

All modeling was performed using FDS version 4 [1, 2]. FDS is a CFD code that was explicitly developed for the purpose of computing fire driven flows. The FDS solver is limited to low Mach number flows (a discussion of this limitation will follow) and for large-scale simulations uses a large-eddy submodel for turbulence. FDS uses a multi-block, Cartesian grid for its solution space. This requires the object being modeled be defined in the input file as a collection of rectangular parallelepipeds (e.g. like it was built from a child's set of building blocks). FDS allows the user to define more than one grid with each grid having a different grid resolution. For example, rather than using a single grid to model an L-shaped room with many grid cells wasted, two grids (one for each leg of the L) could be used without any wasted grid cells.

As a CFD code, FDS produces a tremendous quantity of spatial and temporal output data. A companion visualization tool, Smokeview [3], is available to aid in visualizing FDS results. Smokeview renders 3D dimensional images of the geometry and FDS output data and allows the user to interactively view animations and static images of the FDS output data.

FDS solves a form of the Navier-Stokes equations that eliminate acoustic effects while allowing for large density variations due to temperature or species. As such, the equations are valid for incompressible Mach numbers (Mach < 0.3). All of the scenarios in this study involve releases which are initially sonic (Mach = 1.0). In order to simulate these scenarios with FDS, they were converted to an equivalent low Mach number release. The approach for this is discussed below in 5.2.

4.2 Discussion of Related Validation

The hydrogen releases in this study begin as high momentum jets and transition to buoyancy driven flows. To evaluate the ability of FDS to model a high momentum, horizontal jet, a 130 m/s hydrogen jet into air from a 1 cm orifice with 0.5 cm grid resolution was simulated. The centerline hydrogen concentration and velocity in the momentum region was then compared to an integral jet model [4] based on the method of Badre [5] and the Chen-Rodi correlations [6]. The integral jet model solves the coupled mass, energy and momentum equations for a symmetric jet with a Froude number dependent entrainment rate [7] and the assumption of Gaussian velocity and density profiles in the jet [8, 9]. Figure 3 below shows FDS predicted centerline hydrogen mole fraction and velocity vs. predictions by the integral model.

Extensive validation has been performed of the ability of FDS to predict smoke transport (buoyancy driven flow). The most applicable validation effort to this study involved the simulation of large scale oil fires at the Alaskan North Slope [10]. These experiments documented the wind driven transport over terrain of smoke from a 9 m diameter oil fire. An early version of the FDS flow solver (the computer program ALOFT) was used to simulate these experiments. While this solver has been enhanced to add features such as combustion and radiative heat transfer, a comparison of the flow solver details in [10] with those in [1] show that the essential mass transfer algorithms have not changed. Predictions were shown to match the experiments within the experimental uncertainty. These conditions of weakly buoyant flow over long distances are similar to that of a hydrogen jet once it fully transitions beyond the momentum dominated region.

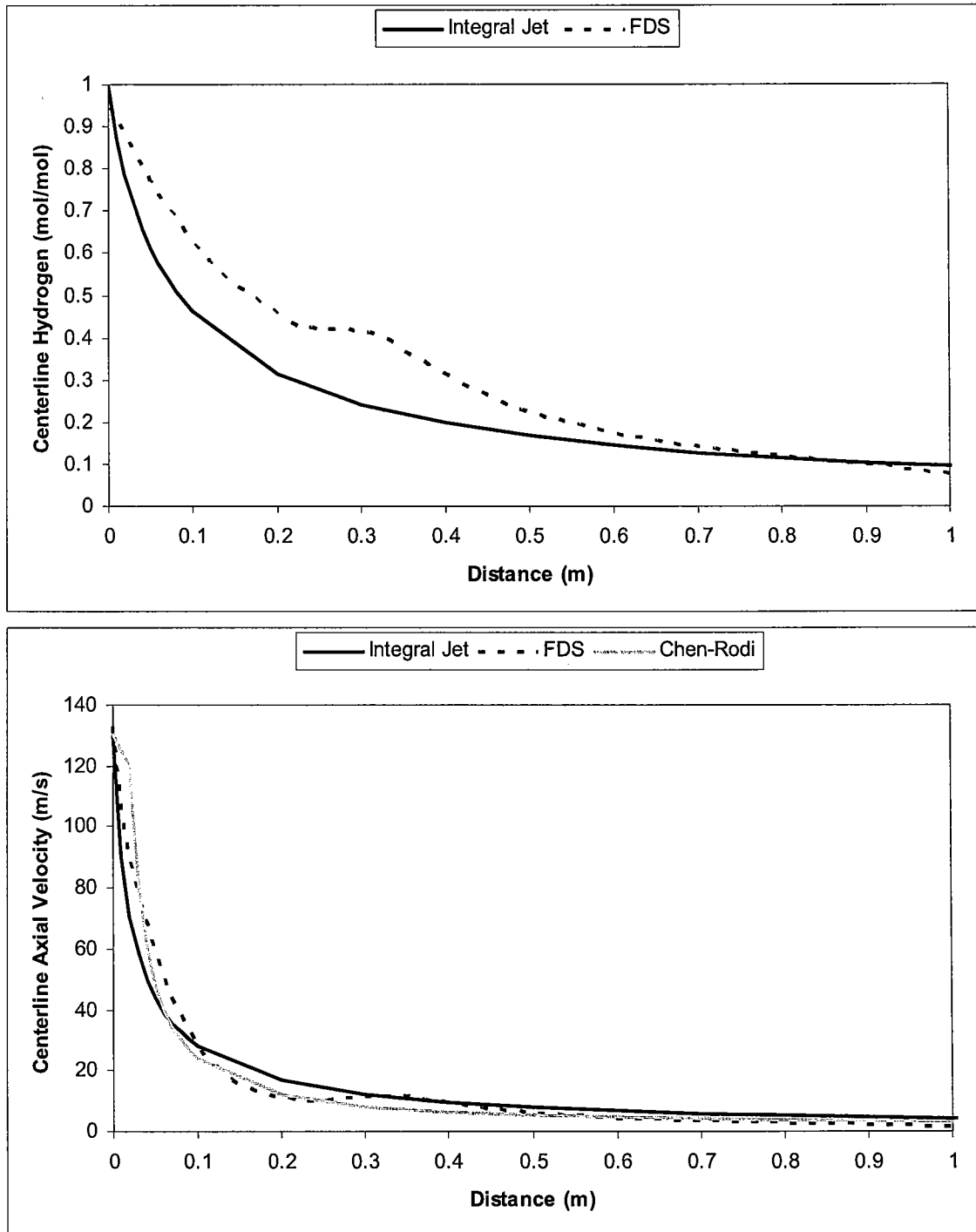


Figure 3: FDS vs. Integral Jet Model and Chen-Rodi Correlations

A 2D, cylindrical coordinates (r - z) version of the FDS solver was used to simulate low-momentum, vertical, helium plumes. The experiment measured the velocity and concentration of a 7.3 cm diameter helium plume into air with an inlet velocity of 45 cm/s [11]. Predictions matched the data low in the plume where rotational entrainment is not a significant factor. This simulation was repeated using FDS v4 in 3D rectangular mode with a 2 mm cm grid containing

2.3 million grid cells. Figure 4 below shows the FDS computed centerline velocity compared with the experimentally measured velocity. The agreement is excellent.

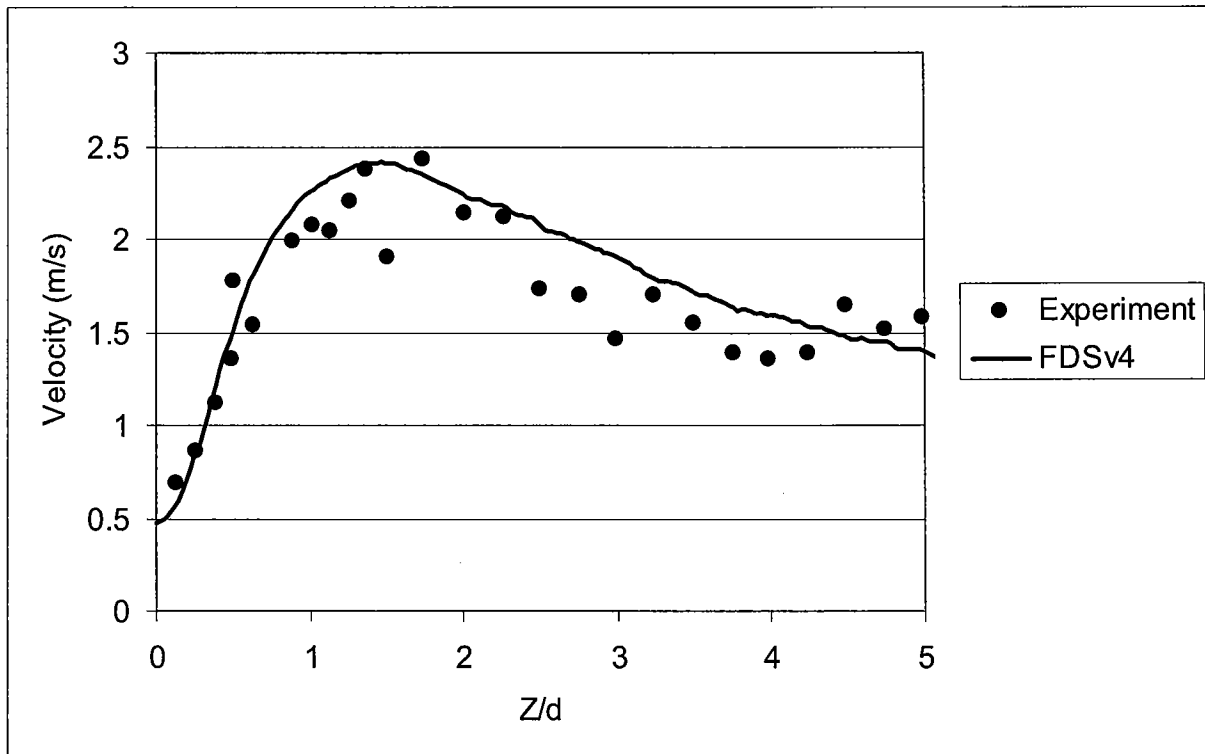


Figure 4: FDS vs. Data for a 7.3 cm Diameter 0.45 m/s Helium Plume

Swain, et. al [12] performed experiments that discharged a 566 L/min, constant flow, horizontal hydrogen jet into air through an 9.45 mm orifice in the center of 2.44 m x 2.44 m aluminum plate. The discharge occurred for 1 minute and measurements of hydrogen concentration were made at six points in the jet for a period of 15 s starting at 45 s. FDS v4 was used to simulate this experiment. The method discussed in section 5.2 was used to create an equivalent jet through a 4.5 cm orifice. An FDS model of the experimental setup was created with a 4 cm grid resolution (4 cm x 4 cm grid cell is equivalent to a 4.4 cm diameter circle) with the jet boundary condition defined as a top-hat profile. A simulation was performed for 60 s. Results of the FDS simulation averaged over 15 s of simulation time starting at 45 s are shown in Figure 5 along with white circles indicating the measurement locations from the test.

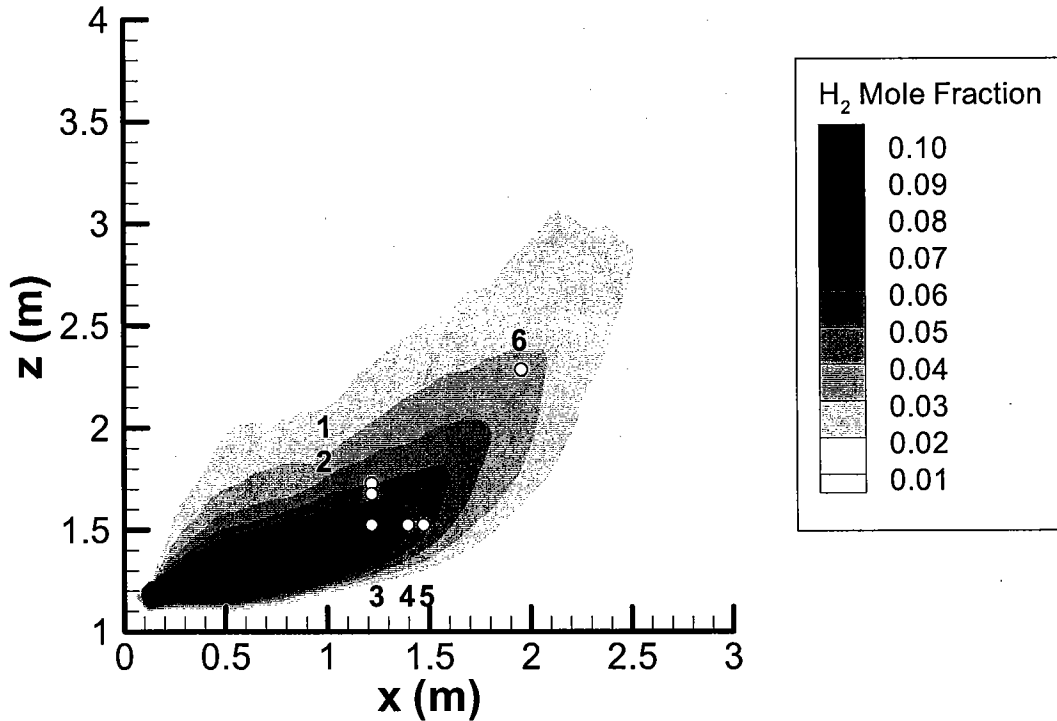


Figure 5: FDS Predictions of a 566 L/min SCFM Hydrogen Jet through a 9.45 mm Orifice

Table 4, below, compares the FDS results with the measured data at each measurement location with the FDS results averaged over the indicated time interval. The numbers on the contour plot indicate the numbering of the measurement points (note the labels for points 1 and 2 are shifted up to improve readability). FDS predictions for measurement locations 1, 2, 5, and 6 show good agreement with the measured data. FDS does not show as steep a gradient between locations 1 and 2 as seen in the data and is underpredicting the hydrogen concentration at locations 3 and 4. FDS is generating slight less buoyancy than was observed during the tests; however, the horizontal extent of the flammable envelope is close to that observed during the test (4 % at position 6). Note that the plume is shown to be fairly steady between 30 s and 60 s as was noted during the tests.

Table 4: FDS Predictions of 20 SCFM Hydrogen Jet vs. Measured Data

Location	Experiment (%)	FDS (30-31 s) (%)	FDS (30-45 s) (%)	FDS (45-46 s) (%)	FDS (45-60 s) (%)
1	5.0-5.9	5.2	5.5	4.3	5.1
2	5.6-7.0	5.8	6.0	5.0	5.6
3	9.4-10.8	7.2	7.8	7.2	7.7
4	8.1-9.4	6.3	6.3	6.5	6.4
5	5.6-6.6	5.9	5.3	5.9	5.7
6	3.5-4.6	2.8	3.0	2.6	3.2

5.0 DESCRIPTION OF FDS SIMULATIONS

5.1 Enclosure Releases

The enclosure releases consisted of two sets of scenarios involving the depressurization of one or more gas cylinders through an orifice. Flow rates of the leaks were computed as a function of time using the gas discharge equations from the EPA Handbook of Chemical Hazard Analysis Procedures [13]. This is a two part function that depends on the pressure of the cylinder relative to the critical pressure required for choked flow. The equations represent an isothermal process. The equation for choked flow is:

$$m = C_d A \sqrt{\gamma P \rho \left(\frac{2}{\gamma - 1} \right)^{\frac{\gamma + 1}{\gamma - 1}}}, \quad (1)$$

where m is the mass flow rate, C_d is the orifice discharge coefficient, P is the tank pressure, P_a is the ambient pressure, ρ is the tank density, A is the leak area, and γ is the ratio of specific heats of the cylinder gas. The equation for non-choked flow is:

$$m = C_d A \sqrt{2P\rho \left(\frac{\gamma}{\gamma - 1} \right) \left[\left(\frac{P_a}{P} \right)^{\frac{2}{\gamma}} - \left(\frac{P_a}{P} \right)^{\frac{\gamma + 1}{\gamma}} \right]}. \quad (2)$$

The non-choked flow equation applies when the cylinder pressure is less than critical pressure, P_{crit} , defined by [14]:

$$P_{crit} = P_a \left(\frac{\gamma + 1}{2} \right)^{\frac{\gamma}{\gamma - 1}}. \quad (3)$$

The two leak types for this set of scenarios are a 0.00635 m diameter leak (PRD failure) from a single bottle pressurized to 450 bar (6530 psi) and an 0.00127 m diameter leak (internal piping failure) with an inventory of three bottles at 450 bar. Using the above equations the time dependent leak rates were computed using Excel and an explicit Euler approach using a 0.2 s time step for the PRD failure and a 10 s time step for the internal piping failure. Results are shown in Figure 6 and Figure 7 below.

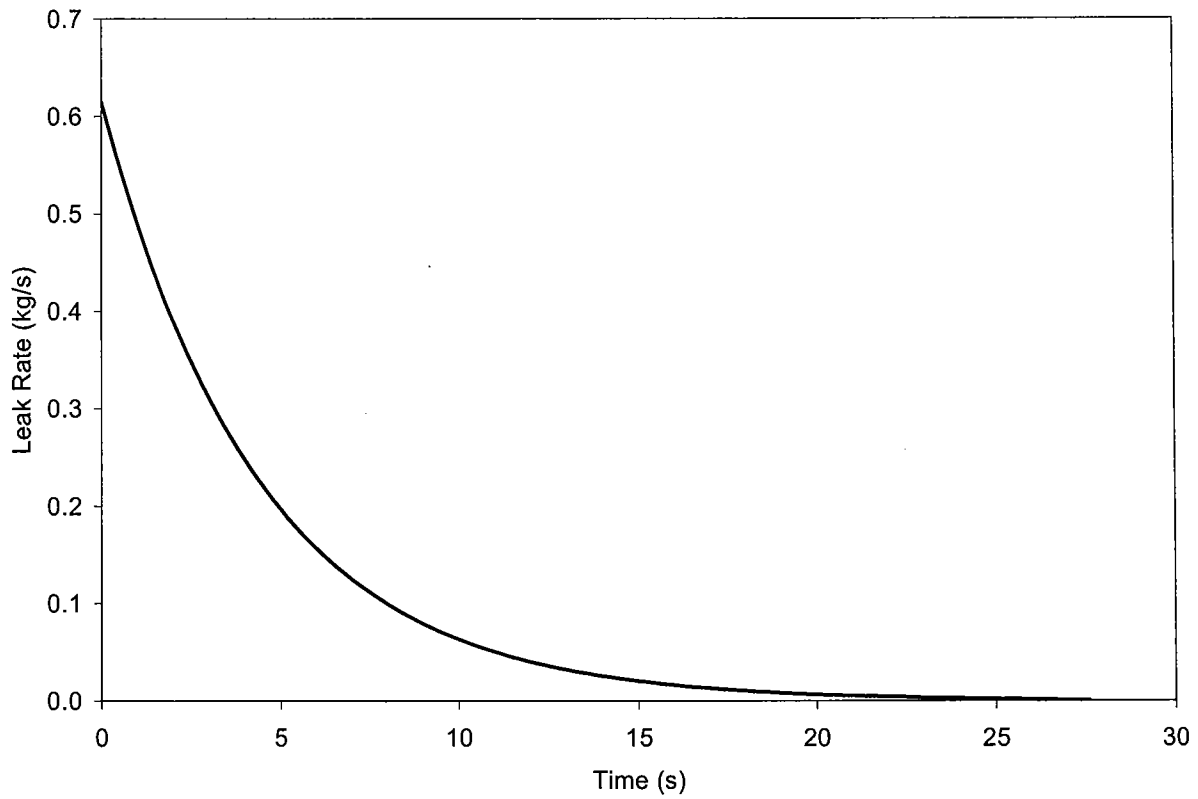


Figure 6: Time Dependent Leak Rate for a Single 450 bar Bottle Emptying Through a 0.00635 m Diameter Leak (PRD Failure)

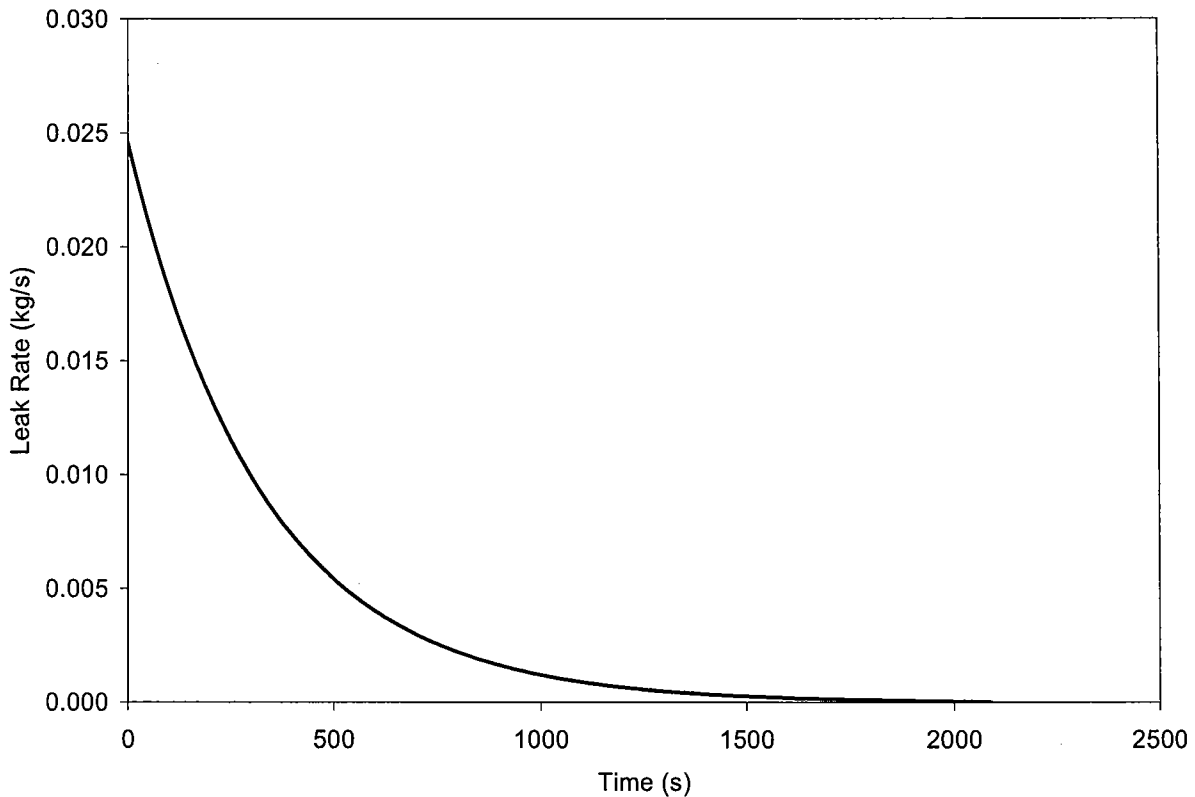


Figure 7: Time Dependent Leak Rate for Three 450 bar Bottles Emptying Through a 0.00127 m Diameter Leak (Internal Piping Failure)

Each leak occurs inside the storage enclosure where it then exits through the enclosure's vent to the ambient. The enclosure vent sizes (from 10 to 40 % of the floor area) are over 1000 times larger than the leak sizes. If the enclosure vent can be used as the release area, then the flows will be low speed from the onset and greatly simplify the simulation. The internal piping leak has an initial mass flux of 0.025 kg/s. In three seconds this leak will emit a volume of hydrogen equal the free air volume of the enclosure (approximately 1 m³). The PRD failure has an initial mass flux of 0.6 kg/s which will equal the free air volume of the enclosure in an eighth of a second. In both cases the reduction in leak rate of the enclosure fill time is small. Therefore, the leak rate is large enough that the enclosure can be considered to instantly fill and vent pure hydrogen from the vent. It is also not necessary to model the enclosure internals for these releases as was noted in Section 2.1.

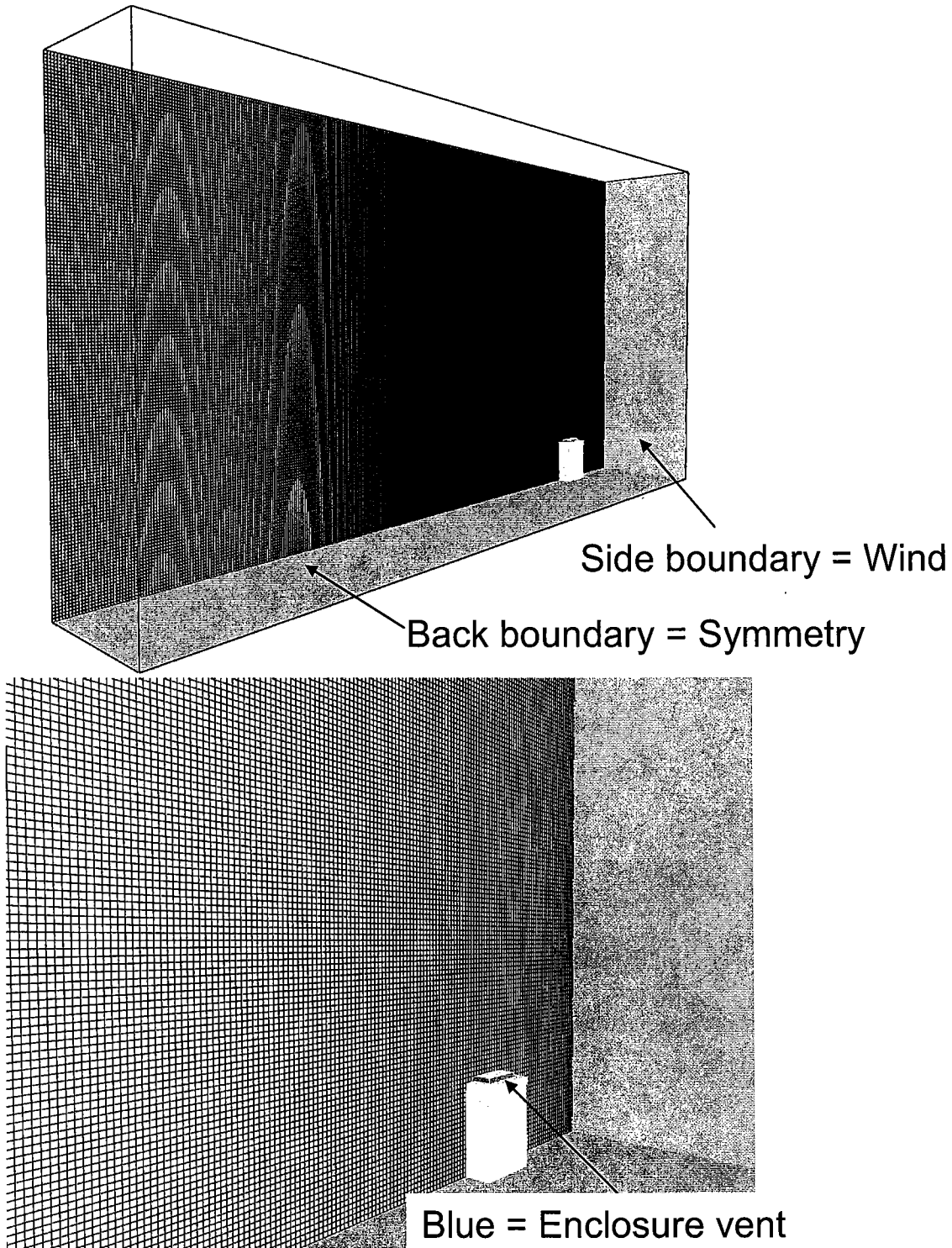


Figure 8: FDS Input Geometry for Internal Leaks

For each scenario of this set an FDS input file was defined that considered the storage enclosure to be a solid obstacle with a vent defined on that obstacle that emitted the appropriate time dependent hydrogen mass flux. The impact of the wind pressure loading on the vent was not

accounted for (i.e. the geometric distribution of the release was constant over the enclosure vent). One boundary of the domain was defined with the desired wind condition, the bottom boundary of the domain was kept solid (the ground), and the remaining boundaries with the exception of the centerline boundary parallel to the wind were defined as open boundary conditions. Since the enclosure is symmetric, a symmetry boundary condition was applied to the centerline boundary parallel to the wind. For both leak rates, a single computational grid was used. However, since the leak rates varied greatly, a larger overall computational domain was required for reasons discussed below for the PRD failure than for the internal piping leak. Thus, the two leak rates had their own computational grid which was used for all simulations of that leak rate. The input geometry is shown in Figure 8 above.

With a larger leak rate, the PRD failures required a larger downstream domain than the small leak. For the PRD failures a 0.08 m grid was used that extended for 28.8 m parallel to the wind boundary and 3.2 m perpendicular and used 2.3 million grid cells. The small leak used a 0.04 m grid that extended 10 m parallel to the wind boundary and 2.4 m perpendicular and used 2.1 million grid cells. For both leaks the computations began with a 10 s period without the leak to establish the wind field solution followed by simulating 10 s of the leak. For the PRD scenarios, 10 s of the leak encompassed the period of time with the maximum volume of hydrogen within its flammable limits. For the small leak, 10 s allowed the formation of the quasi-steady plume that is established during the early stages of the release event (in the first 20 s, the leak rate only drops 5 %).

5.2 Emergency Vent Releases

The second set of scenarios are releases from an emergency vent pipe. The emergency vent is a “T” shaped pipe with an elevation at least 3 m above grade. The cross-piece of the pipe is pointed downwards and the pipe exits are miter cut, see Figure 9 below. The normal of the miter cut must not have a downward component [15]. The worst case release in terms of exposure to the ground will be when the miter cut is such that the exit flow is parallel to ground. A typical vent pipe was defined by the industry panel as a 1” (0.0254 m) diameter pipe.

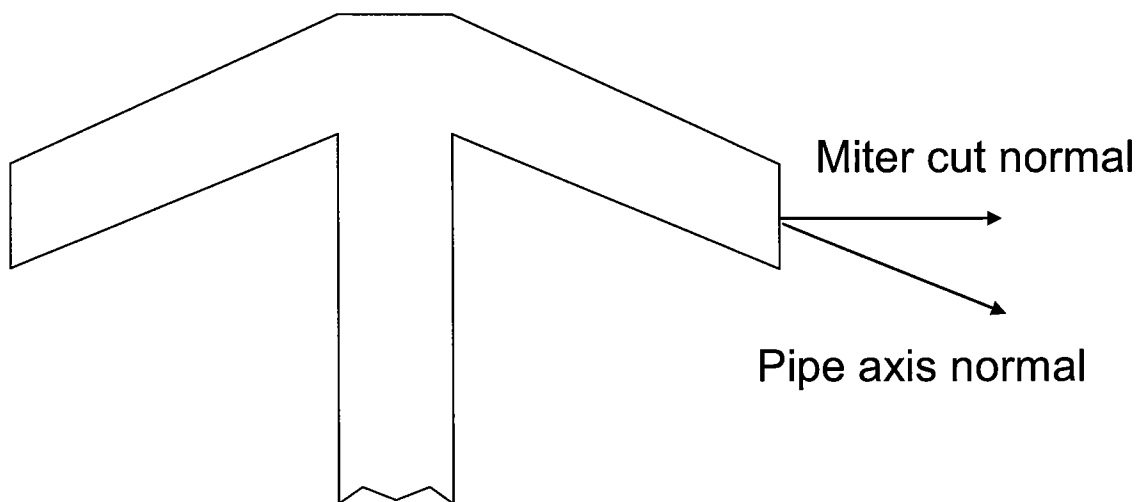


Figure 9: Emergency Vent Pipe Exit

The two leak rates being examined are a constant 70.8 m³/min (regulator failure) and a constant 1.4 m³/min (pinhole leak). Through a 1" pipe these leak rates are hydrogen velocities of 1160 m/s and 23 m/s respectively. The first velocity is sonic and cannot be used directly as an FDS input. The second velocity is subsonic, and could be used directly as an FDS input. However, simulation of a plume from a 1" pipe would require a grid of less than 1". Given the anticipated requirements for the extent of the computational domain, the grid cell requirements to resolve the pipe exit would have exceeded the available computational time and resources.

To transform the emergency vent release flow rates into tractable input for FDS, an application of the conservation of momentum and conservation of mass was performed. Assuming a uniform exit condition the jet momentum is given by the exiting mass flow. The conservation of momentum for the jet is thus given by:

$$U_e^2 \pi r_e^2 \rho_e = U_d^2 \pi r_d^2 \rho_d, \quad (4)$$

where U is the jet velocity, r is the jet radius, ρ is the jet density, and e and d respectively are at the jet exit and a downstream location. The conservation of mass is given by:

$$U_d \pi r_d^2 \rho_d = U_e \pi r_e^2 \rho_e + m_{entr,d}, \quad (5)$$

where $m_{entr,d}$ is the mass entrained by the jet at a downstream location. The downstream velocity will decrease as the jet entrains air. The radius increase and density increase of the jet are functions of the amount of air entrained. By selecting a radius, i.e. setting the grid size by having the jet inlet span 2x2 grid cells, a new jet inlet condition can be defined. Grid sizes of 0.08 m and 0.03 m were selected for the two emergency vent releases. Applying the above equations results in new inlet conditions of 55.2 m/s with hydrogen mass fraction of 0.047 (0.42 mole fraction) for the regulator failure and 4.2 m/s with a hydrogen mass fraction of 0.184 (0.76 mole fraction) for the pinhole leak. The Chen-Rodi jet correlations were then used to determine the downstream distance that gives the desired velocity [5].

$$U_d = \begin{cases} \frac{2r_e U_e 6.2 \sqrt{\frac{\rho_e}{\rho_{air}}}}{x} & \frac{x}{\sqrt{Fr} \left(\frac{\rho_e}{\rho_{air}}\right)^{1/4} 2r_e} < 0.5 \\ \frac{2r_e U_e 7.62 \left(\frac{\rho_e}{\rho_{air}}\right)^{0.45} \left(\frac{2r_e}{x}\right)^{4/5}}{Fr^{1/10}} & 0.5 \leq \frac{x}{\sqrt{Fr} \left(\frac{\rho_e}{\rho_{air}}\right)^{1/4} 2r_e} < 5 \end{cases}, \quad (6)$$

where x is the downstream distance and Fr is the jet Froude number defined as:

$$Fr = \frac{U_e^2}{\frac{g2r_e(\rho_{air} - \rho_e)}{\rho_e}} \quad (7)$$

The downstream distances corresponding to the new inlet conditions are 0.88 m for the regulator failure and 0.30 m for the pinhole leak.

An FDS input file was created that defined two vent sources of hydrogen above the enclosure (one for each of the emergency vent pipe exit branches). It was assumed that the actual vent pipe was located along the enclosure centerline. Thus, the exits were offset based on the distances above. The hydrogen mass fraction and velocity determined by applying the conservation of momentum was applied as a “top-hat” profile to the vent (i.e. uniform across the pipe opening). The same exterior boundary conditions were applied for this case as done for the internal release with the direction of the emergency vent flows parallel to the wind. This would give the worst case condition as the wind could merge the two plumes together and increase the downstream distance at which flammable concentrations would exist.

Since this equivalent source removes a portion of the jet, this portion will need to be included in the analysis. Using the equations above, the distances from the source (100 % hydrogen) to where the average concentration is below either the upper explosive limit and or the upper flammability limit begin can be determined. The mass of hydrogen contained in the region between the either upper limit and the location of the equivalent source is given by the equation below where ΔL is the length of the ignored region between the location where the upper limit occurs and the equivalent source.

$$m = \Delta L \rho_e \pi r_e^2 \quad (8)$$

5.3 External Piping Releases

Two release rates were examined for the external piping releases. There were a 6.9 kg/hr leak and a 4.2 kg/hr leak. There represent the flows of a leak from 150 psig and 85 psig piping respectively through a 0.002 m diameter hole (equivalent diameter of a 20 % hole in 0.375” tubing). Both of these release rates result in sonic conditions. The method discussed in the previous section was used to create new equivalent release conditions. These are respectively 65 m/s with a hydrogen mass fraction of 0.026 (0.38 mole fraction) and 40 m/s with the same mass fraction.

Since these represent leaking from external piping, there is not a known location for the leak. For all the scenarios simulated it was assumed that the leak occurred close to the enclosure on the leeward side.

6.0 DISCUSSION OF DATA ANALYSIS

6.1 FDS Output Postprocessing

Binary data files of hydrogen mole fraction and velocity vectors were stored at regular intervals for the entire domain. FDS is currently distributed with a tool called `fds2ascii` that converts the binary FDS data file to ASCII csv files that can be manipulated within a spreadsheet or other analysis software. The `fds2ascii` source code was modified to create a custom postprocessing of the data files. Each data file was examined to determine the location of all grid cells meeting the following mole fraction criteria: 0.04 to 0.75 (lower and upper flammable limits), 0.06 to 0.75 (modified lower and upper flammable limits), 0.08 to 0.75 (modified lower and upper flammable limits), 0.10 to 0.75 (modified lower and upper flammable limits), and 0.16 to 0.60 (lower and upper explosive limits). The modified lower flammable limits were examined since research has indication that real world releases of hydrogen are difficult to ignite at 4 % hydrogen [12]. Grid cells meeting each criterion were examined to determine if they were part of a larger contiguous volume. Cells meeting the criteria as part of a larger contiguous volume had their masses, volumes, and extents added to a running total. The end result of the post processing was the masses, volumes, and cloud extents for each of the above ranges as a function of time. This data was then used for further analysis. Note the implicit assumption in this analysis that the greatest hazard is given by the contiguous gas cloud rather than small packets of gas within the flammable or explosive limits that might break off from the main cloud.

The regulator failure scenarios resulted in two isolated jets while the pinhole leak scenarios had the upwind jet blown back over the downwind jet. In the former case, where a hazard analysis would postulate a single ignition source, only one jet could ignite. Therefore, the integration discussed above was only performed for the downwind half of the computational domain.

Since the emergency vent and external piping scenarios used an equivalent release, as discussed in Section 5.2, that portion of the release jets not modeled must be included in the analysis.

6.2 Explosion Hazard

The mass of hydrogen within the explosive limits was evaluated using the equivalent TNT method [15]. It was assumed that 10 % of the mass within the limits participated in a detonation. 10 % was selected based on recommendations in the EPA's guide for determining offsite consequences of accidents resulting from clouds of flammable vapors. [22]. The blast wave was evaluated to determine the distances for window breakage (10 % probability at 0.4 psi overpressure), injuries due to flying debris or knock down or damage to single family homes (1 psi overpressure), damage to cinder block structures (2 psi overpressure), and damage to light industrial buildings (4 psi overpressure) [23].

The equivalent TNT method is an approach that allows one the use of the large set of available data on TNT explosions. The energy release of the detonation event, computed as 100 % combustion of 10 % of the mass within the limits, is converted to an equivalent mass of TNT, W . For hydrogen, 1 m³ at standard temperature and pressure is equivalent to 2.02 kg of TNT, or 24.3

kg TNT/kg H₂. A chart is used to obtain a scaled distance, Z , as a function of overpressure. The actual distance, R , is given by:

$$R = ZW^{\frac{1}{3}}. \quad (9)$$

The scaled distances, Z , for 0.4 psi, 1.0 psi, 2.0 psi, and 4.0 psi overpressures are 27.5 m/kg^{1/3}, 16.8 m/kg^{1/3}, 8.1 m/kg^{1/3}, and 4.7 m/kg^{1/3} respectively.

6.3 Burn/Deflagration Hazard

A burn or deflagration poses a hazard by direct thermal contact with the burn or by exposure to the radiative output of the burn. The potential for thermal contact is dictated by the maximum extent of the flammable cloud. Radiative output is function of the maximum heat release rate during the burn. The burn will have two stages. The first stage is ignition and propagation of the burn through the hydrogen cloud resulting from the leak. The second stage is a quasi-steady state burn of the leak at its source. Depending on the leak rate and wind speeds the initial fuel cloud may result in a larger maximum radiative heat flux than the steady-state burn; also, the flux from the cloud will likely expose a larger area, due to the cloud extents, than the flux from the second stage.

A hydrogen flame is a weak emitter of radiation. Since no soot is present in a hydrogen flame, the emission is solely due to band emissions from the water molecules. Hydrogen fires have a measured radiative fraction of 0.17 [24].

For the first stage, a burning cloud of released hydrogen, the radiative output was determined based on the mass of hydrogen within the flammable limits. It was assumed that this hydrogen burned as an unconfined cloud. Assuming the mass of hydrogen is consumed at the end of the cloud lifetime, a point source model was used to compute the distance where an integrated flux of 126 kJ/m² (incipient 2nd degree burns [25]) existed. The analysis assumes that the entire mass within the combustible limits burns. It also assumes the burn is quick enough that cooling mechanisms (convection to the air and advection by wind) are not significant.

For the second stage, the quasi-steady burn at the leak source, the radiative output was computed by first determining the jet flame length and width. The jet flame width, W , and length, L , were determined from the following correlations where M is the jet mass flow rate [27]:

$$L = 20.25M^{0.53}. \quad (10)$$

$$W = 1.52M^{.604}. \quad (11)$$

Then the emissive power was computed by assuming the heat release rate was uniform over a cylinder defined by the aforementioned length and width. A computation of the view factor from the cylinder to a point was then used to compute the distance from the cylinder centerline at

which fluxes of 9.5 kW/m² and 1.6 kW/m² were reached. These values are respectively the API recommended heat fluxes for harm and no harm effects to people [26].

7.0 RESULTS

7.1 Summary of Computations

The FDS outputs from each of the simulations were processed according to the discussions in Section 6.0. From this, the most severe outcome for each scenario and release rate can be determined. Figure 10 through Figure 15 below depict iso-surfaces of hydrogen mole fraction for representative cases of each scenario. The figures show surfaces for 4 % H₂ (LFL), 10 % H₂ (LFL of likely ignition), and 16 % H₂ (LEL). Dimensions of the computational domain are indicated on the figures.

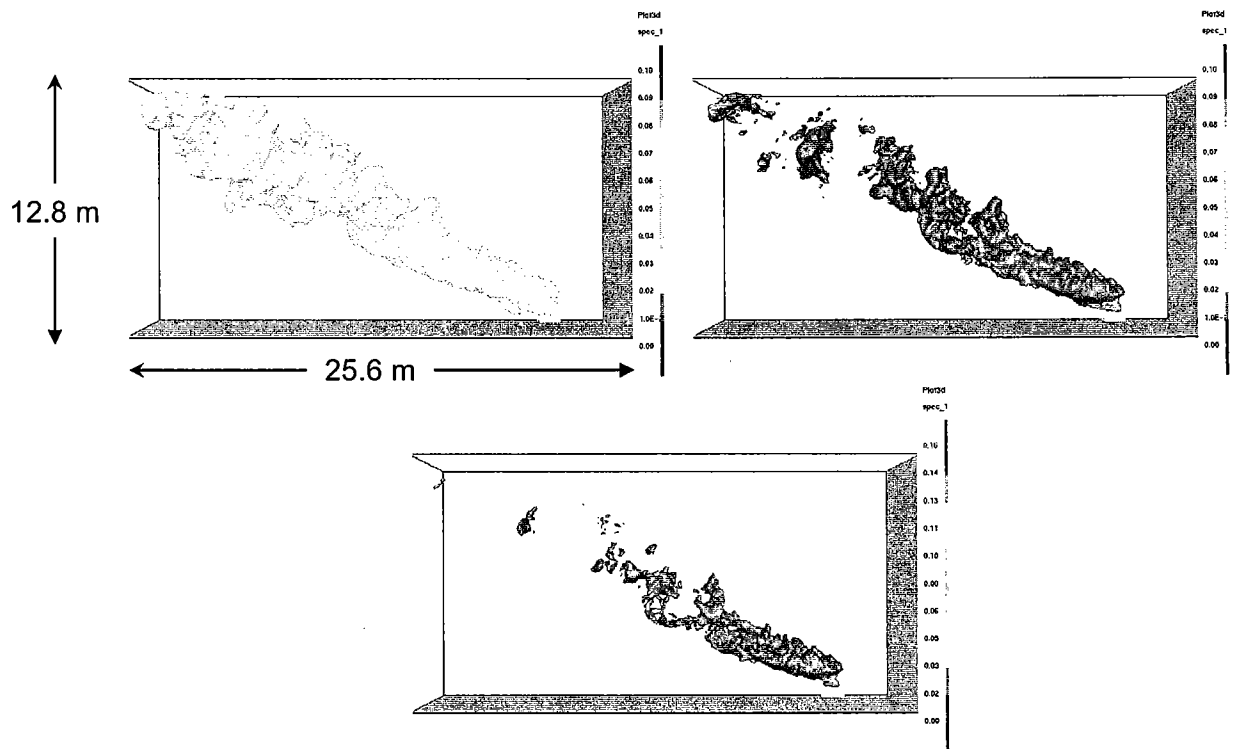


Figure 10: PRD Failure, 0.4 Vent Size, Perpendicular 2.2 m/s Wind

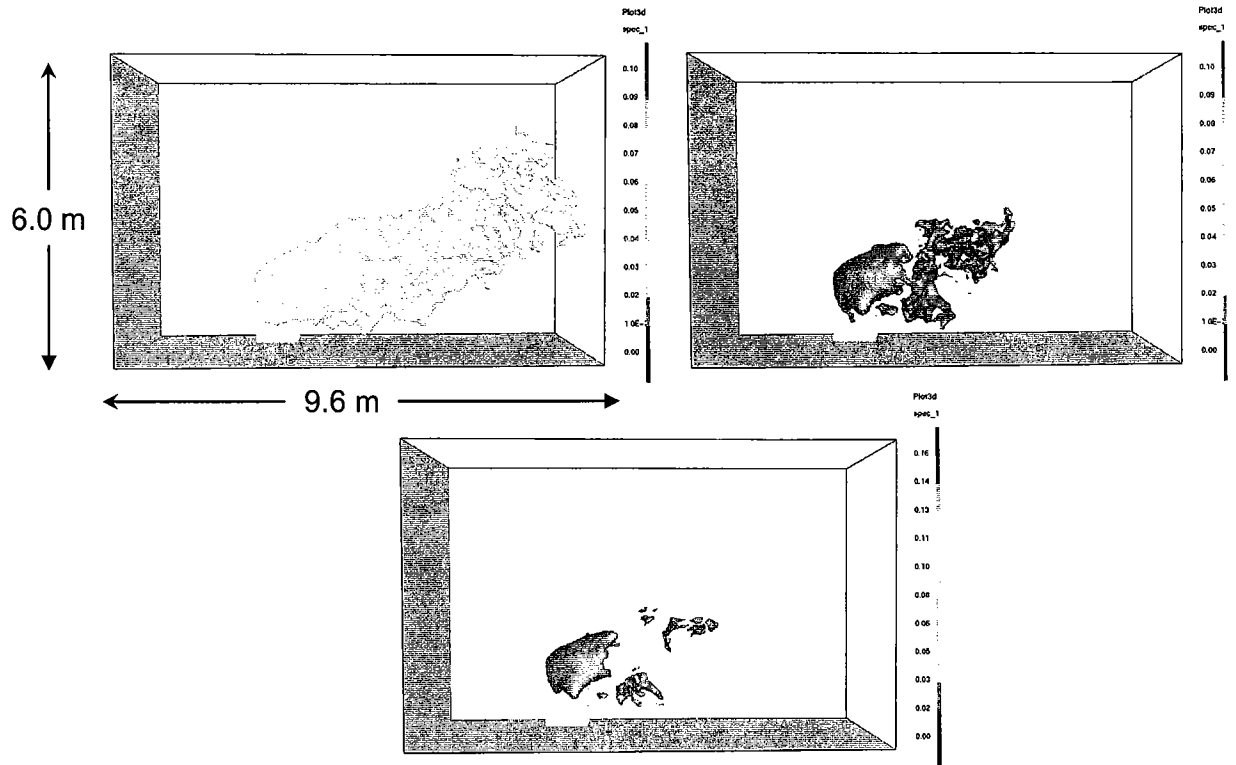


Figure 11: Internal Piping Leak, Face Vent

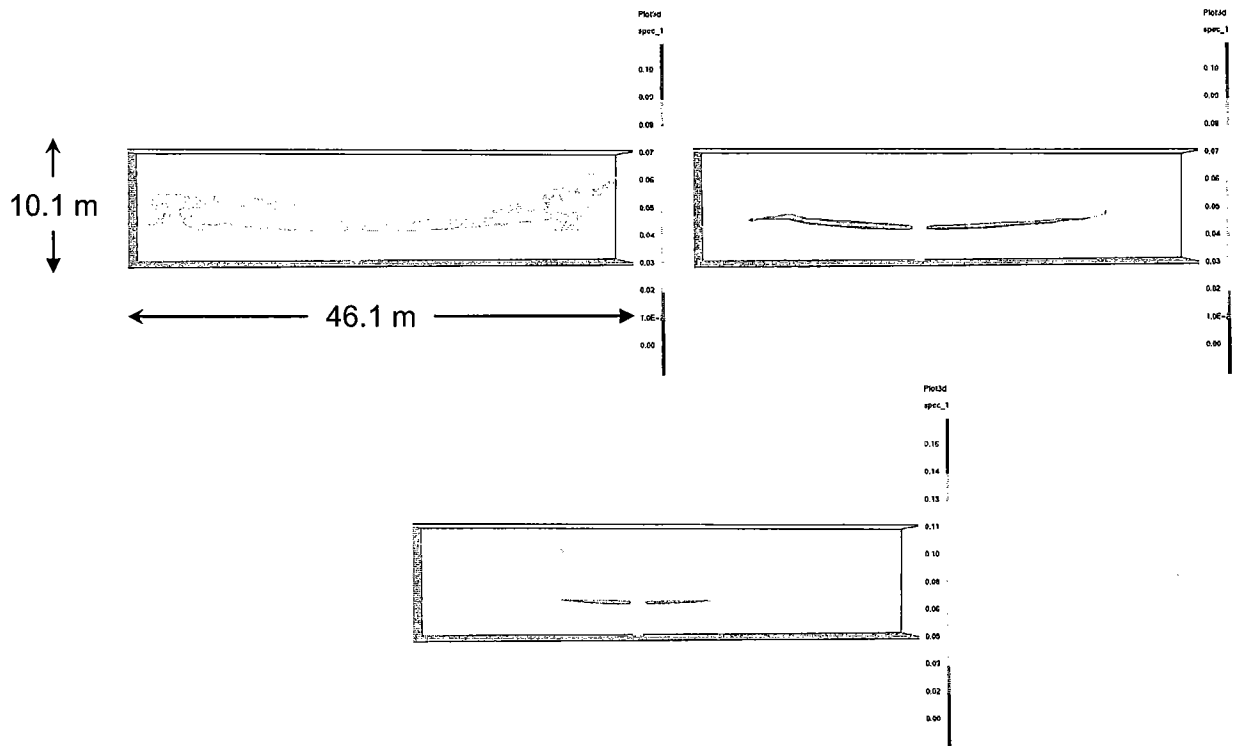


Figure 12: Emergency Vent of Regulator Failure, 2.2 m/s Wind

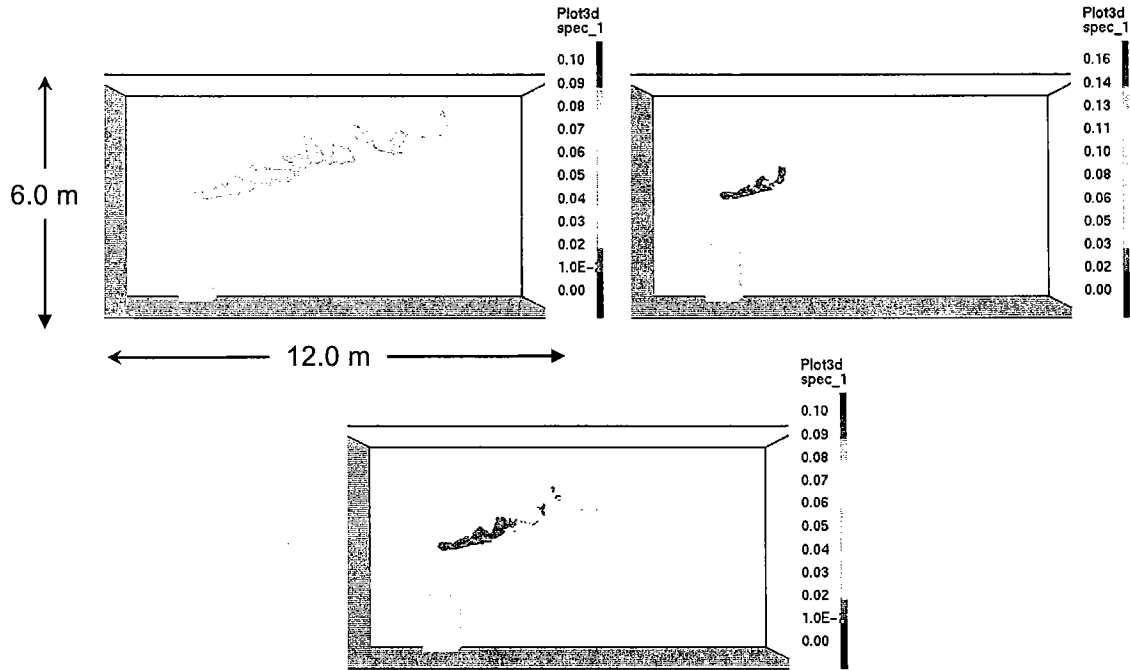


Figure 13: Emergency Vent of Pinhole Leak, 2.2 m/s Wind

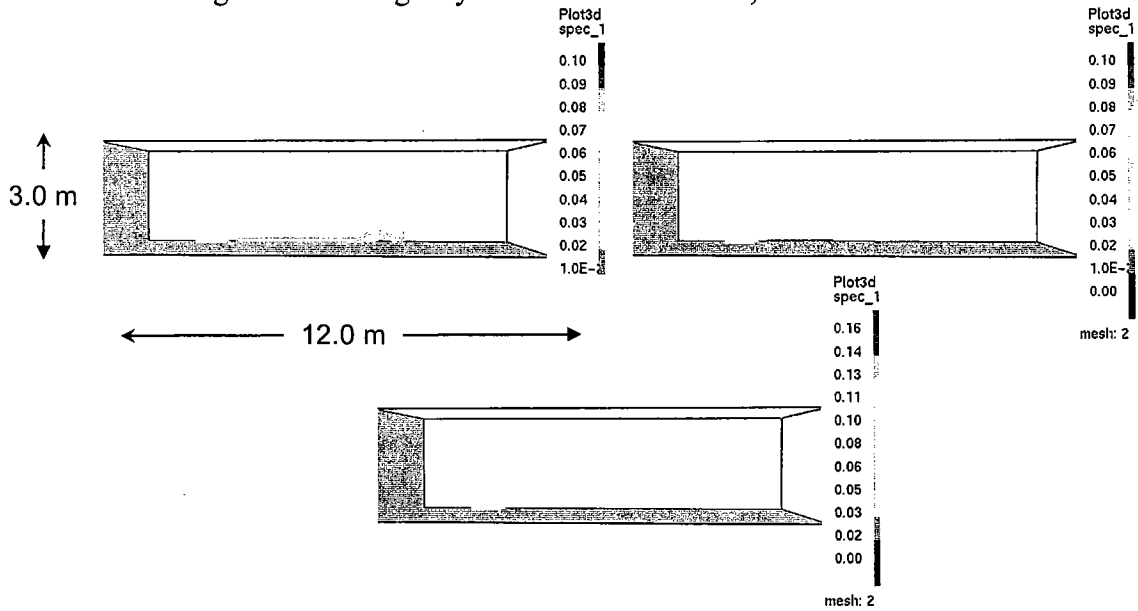


Figure 14: Ground Level 150 psig Pipe Leak, 2.2 m/s Wind

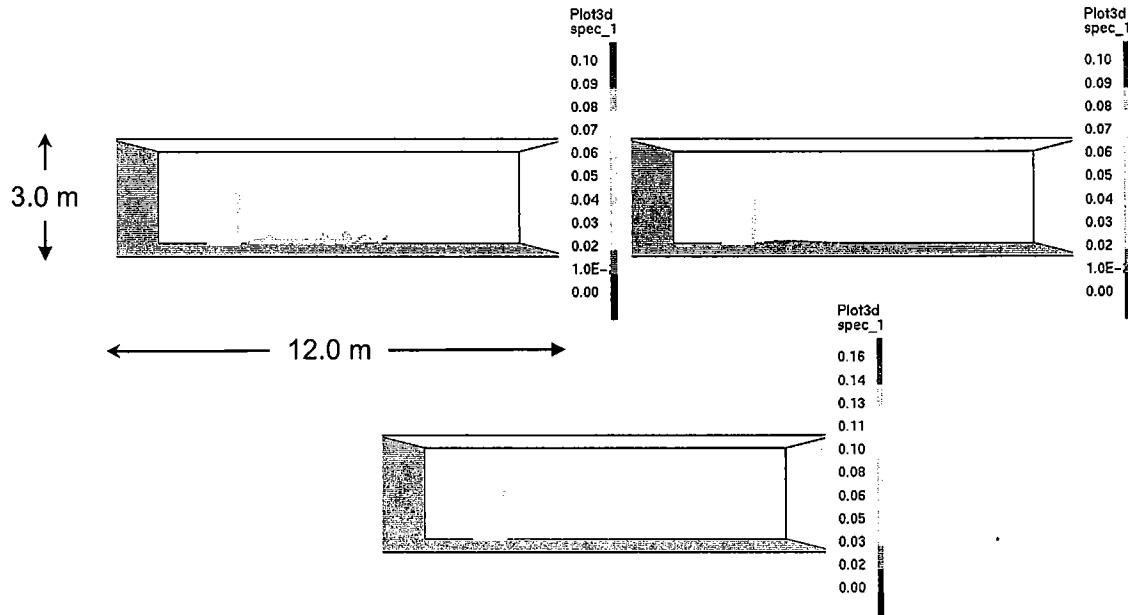


Figure 15: Ground Level 85 psig Pipe Leak, 2.2 m/s Wind

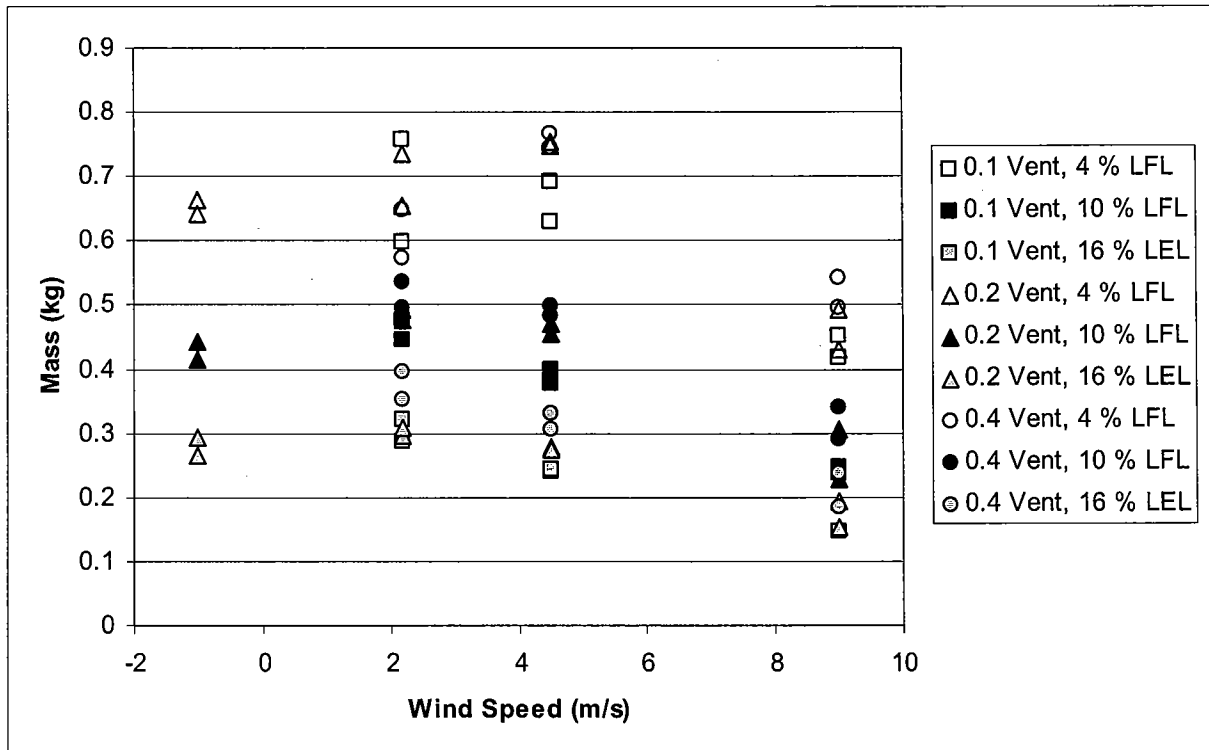


Figure 16: Scatter Plot of the Hydrogen Mass between the LFL and UFL and the LEL and the UEL for the Ridge Vent PRD Failure Scenarios (-1 m/s Wind = Sinusoidal Wind Speed)

Figure 16 above shows a scatter plot of the results for the PRD failure with a ridge vent on the enclosure; both parallel and perpendicular wind directions are plotted. The figure shows that vent size has a small impact on the hazard from the release. Wind direction also has a small impact on the hazard from the release as can be seen by observing the identical symbols at the various wind speed. Wind speed has a more significant impact on the hazard than the other variables.

Figure 17 below shows a scatter plot of all of the external pipe leak results. The wind speed of -1 indicates the sinusoidal wind profile. There is a significant difference in the hazard for ground level leak vs. a slightly elevated leak. Wind speed has a similar impact to that observed for the enclosure ridge vent results shown in Figure 16.

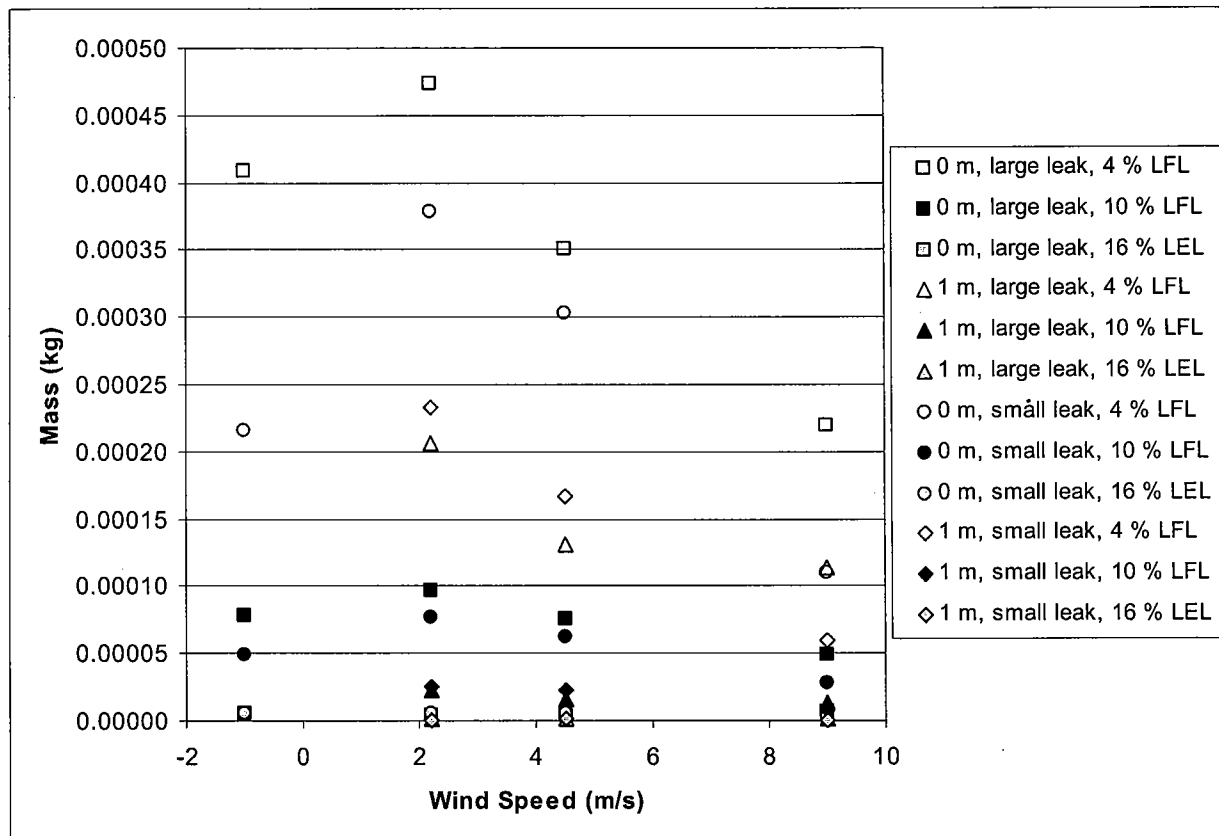


Figure 17: Scatter Plot of the Hydrogen Mass between the LFL and UFL and the LEL and the UEL for the for the External Pipe Leak Scenarios (-1 m/s Wind = Sinusoidal Wind Speed)

7.2 Explosion

The results of performing the equivalent TNT computation are shown in Table 5 through Table 7 below. The distances represent the pressure distance computed using Equation 9 added to 50 % of the cloud extent (the explosion was assumed to occur in the center of the gas cloud). The worst case scenarios are those with large leak rates internal to the enclosure. The PRD failure creates a hydrogen cloud that if it detonated could damage windows at 37 m, injure people at 27

m, damage homes at 18 m, and industrial structures at 14 m. However, this cloud does not persist for a long period of time and within 10 s the hazard distances drop to 14.5 m, 9.1 m, 4.8 m, and 3.0 m. The internal release of a small leak that empties three bottles has hazard distances of 11 m, 8 m, 6 m, and 5 m. These conditions will persist for an extended period of time, minutes vs. seconds for the PRD failure.

The external piping scenarios present the smallest hazard. Leaks at ground level present a larger hazard due to reduced entrainment and dilution of the hydrogen. For the selected leak rates and wind speeds the leak elevation was the dominant parameter in determining the hazard. The PRD failure creates a hydrogen cloud that if it detonated could damage windows at 1.6 m, injure people at 1.3 m, damage homes at 1.1 m, and damage industrial structures at 0.7 m. The corresponding distances for the elevated leaks are 1.0 m, 0.9 m, 0.7 m, and 0.7 m.

Table 5: Explosion Results Matrix for Internal Release

Inventory (bottles)	Wind Speed (m/s)	Vent Location	Vent Area (m ² vent/ m ² floor area)	Wind Direction with Respect to Vent	Wind Variation	Distance (m)			
						0.4 psi	1.0 psi	2.0 psi	4.0 psi
1 (PRD)	2.2	Ridge-line	0.10	Parallel	None	32.1	22.3	14.3	11.2
			0.10	Perpendicular		30.0	20.5	12.8	9.8
			0.22	Parallel		30.8	21.2	13.4	10.4
			0.22	Perpendicular		31.8	22.1	14.1	11.0
			0.40	Parallel		32.5	22.4	14.1	10.9
			0.40	Perpendicular		34.4	23.9	15.3	12.0
	4.5		0.10	Parallel		33.5	24.6	17.3	14.5
			0.10	Perpendicular		34.3	25.4	18.1	15.2
			0.22	Parallel		35.1	25.7	18.1	15.1
			0.22	Perpendicular		34.1	24.8	17.2	14.3
			0.40	Parallel		36.3	26.7	18.8	15.7
			0.40	Perpendicular		37.0	27.1	18.9	15.8
	9.0		0.10	Parallel		29.1	21.5	15.3	12.9
			0.10	Perpendicular		28.7	21.1	14.9	12.5
			0.22	Parallel		31.3	23.0	16.2	13.6
			0.22	Perpendicular		28.6	20.9	14.7	12.2
			0.40	Parallel		29.0	20.8	14.1	11.5
			0.40	Perpendicular		29.9	21.1	13.8	11.0
3 (Piping)	2.2	Ridge-line	0.10	Parallel	None	11.1	8.0	5.5	4.5
			0.10	Perpendicular		11.0	7.9	5.3	4.2
			0.22	Parallel		10.7	7.5	4.9	3.8
			0.22	Perpendicular		11.4	8.0	5.3	4.2
			0.40	Parallel		10.7	7.5	4.9	3.9
			0.40	Perpendicular		11.3	8.1	5.4	4.4
	4.5		0.10	Parallel		8.8	6.1	4.0	3.1
			0.10	Perpendicular		10.6	7.7	5.3	4.3
			0.22	Parallel		9.5	6.6	4.3	3.4
			0.22	Perpendicular		10.5	7.6	5.2	4.2
			0.40	Parallel		9.1	6.3	4.1	3.2
			0.40	Perpendicular		10.3	7.5	5.1	4.2
	9.0		0.10	Parallel		8.3	6.0	4.2	3.5
			0.10	Perpendicular		6.4	4.3	2.6	1.9
			0.22	Parallel		6.9	4.7	3.0	2.3
			0.22	Perpendicular		7.1	4.9	3.1	2.4
			0.40	Parallel		7.4	5.3	3.6	2.9
			0.40	Perpendicular		5.3	3.5	2.0	1.4
1 (PRD) 3 (Piping)	4.5	Face	0.1	Parallel	Sinusoidal 0.3 Hz ± 2 m/s	35.1	25.7	18.1	15.1
Perpendicular				35.1		26.0	18.5	15.5	
Parallel				13.1		9.3	6.2	5.0	
Perpendicular				10.5		7.8	5.5	4.7	
1 (PRD) 3 (Piping)	4.5	Ridge-line	0.2	Parallel	Sinusoidal 0.3 Hz ± 2 m/s	33.0	23.5	15.7	12.7
Perpendicular				32.0		22.8	15.3	12.3	
Parallel				10.5		7.5	5.1	4.1	
Perpendicular				8.3		5.1	2.5	1.4	

Table 6: Explosion Results Matrix for Emergency Vent Release

Failure Mode	Leak Rate (m ³ /min)	Wind Speed (m/s)	Wind Variation	Distance (m)			
				0.4 psi	1.0 psi	2.0 psi	4.0 psi
Regulator	70.8	2.2	None	8.1	6.3	4.8	4.3
		4.5		7.3	5.7	4.4	3.9
		9.0		6.5	5.1	3.8	3.4
Pinhole	1.4	2.2		4.9	3.8	3.0	2.7
		4.5		4.9	4.0	3.2	2.9
		9.0		3.5	2.8	2.2	2.0
Regulator	70.8	4.5	Sinusoidal 0.3 Hz ± 2 m/s	7.2	5.6	4.3	3.7
Pinhole	1.4			5.0	4.0	3.2	2.9

Table 7: Explosion Results Matrix for Release from External Piping

Pipe (psig)	Leak Rate (kg/hr)	Wind Speed (m/s)	Leak Height (m)	Wind Variation	Distance (m)				
					0.4 psi	1.0 psi	2.0 psi	4.0 psi	
85	4.2	2.2	0	None	1.5	1.3	1.1	1.0	
			1		1.0	0.9	0.7	0.7	
		4.5	0		1.5	1.3	1.1	1.0	
			1		1.0	0.9	0.7	0.7	
		9.0	0		1.4	1.2	1.1	1.0	
			1		1.0	0.9	0.8	0.7	
150	6.9	2.2	0		None	1.5	1.3	1.1	1.0
			1			1.0	0.9	0.7	0.7
		4.5	0			1.5	1.3	1.1	1.0
			1			1.0	0.9	0.7	0.7
		9.0	0			1.6	1.3	1.1	1.0
			1			1.0	0.9	0.8	0.7
85	4.2	4.5	0	Sinusoidal 0.3 Hz ± 2 m/s		1.5	1.3	1.1	1.0
150	6.9					1.5	1.3	1.1	1.0

7.3 Burn/Deflagration Results

The following three tables show grouped by release source the maximum extent of the hydrogen gas cloud for each scenario simulated. The distance shown is the downstream distance in meters from the centerline the enclosure. The distance is shown for the flammable gas volume above 4 %, the flammable gas volume above 10 %, and the detonatable gas volume above 16 %. This distance is not a contiguous cloud distance; rather it is the distance at which packets of gas at exceed the limits over a span of at least three grid cells.

Table 8: Plume Extents Results Matrix for Internal Release

Inventory (bottles)	Wind Speed (m/s)	Vent Location	Vent Area (m ² vent/ m ² floor area)	Wind Direction with Respect to Vent	Wind Variation	Distance (m)		
						4 % LFL	10 % LFL	16 % LEL
1 (PRD)	2.2	Ridge-line	0.10	Parallel	None	13.7	13.7	13.7
			0.10	Perpendicular		14.7	14.7	11.2
			0.22	Parallel		14.6	14.5	12.3
			0.22	Perpendicular		14.7	14.7	13.5
			0.40	Parallel		14.6	14.6	12.8
			0.40	Perpendicular		14.7	14.7	14.6
	4.5		0.10	Parallel		22.9	22.8	21.1
			0.10	Perpendicular		23.0	23.0	22.5
			0.22	Parallel		22.9	22.6	21.9
			0.22	Perpendicular		23.0	22.1	20.3
			0.40	Parallel		22.9	22.9	22.9
			0.40	Perpendicular		23.0	23.0	22.8
	9.0		0.10	Parallel		26.2	21.4	19.2
			0.10	Perpendicular		26.2	26.2	18.3
			0.22	Parallel		28.8	23.7	19.8
			0.22	Perpendicular		26.2	22.7	17.7
			0.40	Parallel		26.2	22.2	15.9
			0.40	Perpendicular		26.2	26.2	14.1
3 (Piping)	2.2	0.10	Parallel	7.2	7.1	6.2		
		0.10	Perpendicular	7.2	7.2	5.7		
		0.22	Parallel	7.2	7.0	4.8		
		0.22	Perpendicular	7.2	7.2	5.5		
		0.40	Parallel	7.2	6.3	4.9		
		0.40	Perpendicular	7.2	7.2	5.9		
	4.5	0.10	Parallel	7.2	5.6	3.9		
		0.10	Perpendicular	7.2	7.0	6.0		
		0.22	Parallel	7.2	5.2	4.2		
		0.22	Perpendicular	7.2	7.0	5.9		
		0.40	Parallel	7.2	5.3	4.0		
		0.40	Perpendicular	7.2	6.0	5.9		
	9.0	0.10	Parallel	7.2	5.1	4.9		
		0.10	Perpendicular	6.5	3.6	2.0		
		0.22	Parallel	6.9	5.0	2.8		
		0.22	Perpendicular	7.1	4.7	2.8		
		0.40	Parallel	6.9	4.6	4.0		
		0.40	Perpendicular	2.6	1.7	1.2		
1 (PRD) 3 (Piping)	4.5	Face	0.10	Parallel	None	22.9	22.6	21.9
Perpendicular				23.0		23.0	23.0	
Parallel				7.2		7.2	6.7	
Perpendicular				7.2		7.2	6.9	
1 (PRD) 3 (Piping)	4.5	Ridge-line	0.22	Parallel	Sinusoidal 0.3 Hz ± 2 m/s	28.8	21.6	16.9
Perpendicular				26.2		23.7	16.5	
Parallel				7.2		6.4	5.6	
Perpendicular				7.2		6.6	5.8	

Table 9: Plume Extents Results Matrix for Emergency Vent Release

Failure Mode	Leak Rate (m ³ /min)	Wind Speed (m/s)	Wind Variation	Distance (m)		
				4 % LFL	10 % LFL	16 % LFL
Regulator	70.8	2.2	None	25.5	21.6	7.0
		4.5		25.5	20.4	6.4
		9.0		25.5	14.4	5.4
Pinhole	1.4	2.2		8.7	5.8	4.4
		4.5		9.6	8.5	4.9
		9.0		9.3	5.0	3.4
Regulator	70.8	4.5	Sinusoidal 0.3 Hz ± 2 m/s	25.5	18.5	6.0
Pinhole	1.4			9.2	5.6	4.8

Table 10: Plume Extents Results Matrix for Release from External Piping

Pipe (psig)	Leak Rate (kg/hr)	Wind Speed (m/s)	Leak Height (m)	Wind Variation	Distance (m)		
					4 % LFL	10 % LFL	16 % LFL
85	4.2	2.2	0	None	5.6	3.1	0.7
			1		3.8	1.7	0.1
		4.5	0		2.9	2.3	0.6
			1		2.2	1.2	0.2
		9.0	0		1.5	1.5	0.5
			1		1.3	0.7	0.2
150	6.9	2.2	0		9.1	4.5	0.5
			1		3.9	1.5	0.1
		4.5	0		6.9	3.1	0.5
			1		2.5	1.3	0.1
		9.0	0		2.6	2.0	0.8
			1		1.6	0.9	0.2
85	4.2	4.5	0	Sinusoidal 0.3 Hz ± 2 m/s	2.8	2.2	0.7
150	6.9				5.3	2.7	0.6

Table 11 through Table 13 below summarize the distances at which total radiative fluences of 126 kJ/m² would result from a cloud deflagration. These distances represent the sum of the radiative distance for a point source cloud combined with 50 % of the cloud extents (ignition is assumed at the cloud center). Table 14 shows the distances at radiative fluxes of 9.5 kW/m² and 1.6 kW/m² are anticipated from a quasi-steady burn.

Table 11: Radiative Results Matrix for Internal Release

# of bottles	Wind Speed (m/s)	Vent Location	Vent Area (m ² vent/ m ² floor area)	Wind Direction with Respect to Vent	Wind Variation	Burn Distance (m)	
						4 % LFL	10 % LFL
1 (PRD)	2.2	Ridge-line	0.10	Parallel	None	9.9	9.5
			0.10	Perpendicular		10.7	9.9
			0.22	Parallel		10.4	9.9
			0.22	Perpendicular		10.7	10.1
			0.40	Parallel		10.2	10.0
			0.40	Perpendicular		10.5	10.2
	4.5		0.10	Parallel		14.7	13.9
			0.10	Perpendicular		14.6	13.9
			0.22	Parallel		14.8	14.0
			0.22	Perpendicular		14.9	13.7
			0.40	Parallel		14.8	14.2
			0.40	Perpendicular		14.9	14.3
	9.0		0.10	Parallel		15.7	12.6
			0.10	Perpendicular		15.6	15.0
			0.22	Parallel		17.1	14.0
			0.22	Perpendicular		15.7	13.2
			0.40	Parallel		15.8	13.2
			0.40	Perpendicular		16.0	15.4
3 (Piping)	2.2	Ridge-line	0.10	Parallel	None	4.6	4.3
			0.10	Perpendicular		4.1	4.0
			0.22	Parallel		4.4	4.1
			0.22	Perpendicular		4.4	4.2
			0.40	Parallel		4.4	4.1
			0.40	Perpendicular		4.4	4.2
	4.5		0.10	Parallel		4.4	3.7
			0.10	Perpendicular		4.4	4.1
			0.22	Parallel		4.2	3.2
			0.22	Perpendicular		4.2	4.0
			0.40	Parallel		4.2	3.0
			0.40	Perpendicular		4.2	4.0
	9.0		0.10	Parallel		4.2	3.1
			0.10	Perpendicular		4.2	3.4
			0.22	Parallel		4.0	2.9
			0.22	Perpendicular		3.6	2.1
			0.40	Parallel		3.8	2.8
			0.40	Perpendicular		3.9	2.7
1 (PRD)	4.5	Face	0.1	Parallel	None	14.8	14.0
3 (Piping)				Perpendicular		14.7	14.0
3 (Piping)				Parallel		4.6	4.3
1 (PRD) 3 (Piping)	4.5	Ridge-line	0.2	Parallel	Sinusoidal 0.3 Hz ± 2 m/s	17.6	13.4
				Perpendicular		16.2	14.4
				Parallel		4.2	3.7
				Perpendicular		4.2	3.8

Table 12: Radiative Results Matrix for Emergency Vent Release

Failure Mode	Leak Rate (m ³ /min)	Wind Speed (m/s)	Wind Variation	Burn Distance (m)	
				4 % LFL	10% LFL
Regulator	70.8	2.2	None	13.6	11.2
		4.5		13.5	10.6
		9.0		13.3	7.5
Pinhole	1.4	2.2		4.5	3.0
		4.5		5.0	4.4
		9.0		4.7	2.6
Regulator	70.8	4.5	Sinusoidal 0.3 Hz ± 2 m/s	13.5	9.6
Pinhole	1.4			4.7	2.9

Table 13: Radiative Results Matrix for Release from External Piping

Pipe (psig)	Leak Rate (kg/hr)	Wind Speed (m/s)	Leak Height (m)	Wind Variation	Burn Distance (m)	
					4 % LFL	10 % LFL
85	4.2	2.2	0	None	0.24	0.11
			1		0.19	0.06
		4.5	0		0.21	0.10
			1		0.16	0.06
		9.0	0		0.13	0.06
			1		0.10	0.03
150	6.9	2.2	0		0.27	0.12
			1		0.18	0.06
		4.5	0		0.23	0.11
			1		0.14	0.05
		9.0	0		0.18	0.09
			1		0.13	0.05
85	4.2	4.5	0	Sinusoidal 0.3 Hz ± 2 m/s	0.18	0.09
150	6.9			0.25	0.11	

Table 14: Radiative Results Matrix for Quasi-steady Burning at Leak Source

Leak		Distance (m)	
		9.5 kW/m ²	1.6 kW/m ²
Internal	PRD Failure	11.2	28.
	Internal Piping	2.2	5.6
Emergency Vent	Regulator	4.5	11.
	Pinhole Leak	0.6	1.6
External Piping	150 psig leak	0.6	1.5
	85 psig leak	0.5	1.2

7.4 Alternate Enclosure Scenario

A question regarding the use of a PRD failure as the basis for siting distances was raised during the project. It arose due to the results of the current study pointing to larger siting distances than are currently required for flammable gas storage. In an effort to examine this issue further two additional PRD failure simulations were performed. Each simulation assumed the same size PRD and gas bottle; however, a storage pressure of 2400 psi was assumed and ethylene (neutrally buoyant) was simulated in addition to hydrogen. Table 15 below compares the results of the additional computations with the worst case failure mode simulated in the initial scenario matrix. The results of the table, the large distances for ethylene, suggest that the large flow rates from a PRD failure were not considered when setting other flammable gas siting requirements. The PRD failure (at least without accounting for probability of occurrence) may not be an appropriate scenario for siting requirements.

Table 15: Results of Lower Pressure and Alternate Gas Simulations

Category	Sub-category	Distance (m)		
		6500 psi H ₂	2400 psi H ₂	2400 psi C ₂ H ₄
Detonation	Glass	36.3	24.9	37.9
	Injury	26.7	18.0	24.0
	Structure	15.7	10.2	8.1
Cloud Limits	LFL	22.9	4.8	14.7
Deflagration	4 % LFL	17.6	4.5	14.9
	10 % LFL	13.4	3.6	12.5
Quasi-steady	9.5 kW/m ²	11.2	6.8	17.4
	1.6 kW/m ²	28.1	17.0	43.7

8.0 CONCLUSIONS

The worst possible leak scenario is a PRD failure within the enclosure. Flammable mixtures for this scenario can be found at distances close to 30 m from the enclosure. A detonation of the gas volume could cause glass breakage at distances of 37 m, injury to people at distances of 27 m, and structural failure at distances of 14 m. Radiative fluxes could cause potential ignition at 11 m and skin pain at 28 m; however, it is noted that the duration of this event is very short and

within 10 s these distances drop to 3.6 m and 9.0 m. If a PRD failure is believed a likely enough scenario, then it will likely drive the distance requirements for NFPA 55.

Ignoring the PRD failure mode, the remaining failure modes are all relatively low flow rates in comparison; however, the jet formed by the emergency vent flow due a regulator failure is almost as large as that from the PRD failure, 25 m vs. 30 m for the PRD. However, the volume of the regulator failure jet is much smaller than that of the PRD failure and emergency vent's higher elevation will reduce the risk to people and ground level equipment and structures. Leaks from external piping can form a jet that extends up to 10 m and can directly impinge upon people or equipment at ground level. The largest explosion hazard is posed by the internal piping leak with glass breakage at distances of 13m, injury to people at distances of 9 m, and structural failure at distances of 5 m. The regulator failure through the emergency vent results in the greatest radiative threat with ignition possible at 5 m, skin pain from the jet at 11 m, and flash burns from the clouds at 14 m. Unlike the PRD failure, the regulator failure may last for an extended period of time if it were to burn would pose a higher risk of igniting remote targets.

Table 16 summarizes the minimum distances at which an effect is seen by a number of different targets. The effect can be either damage or injury due to overpressure or damage or injury due to actual or potential thermal effects. Two sets of distances are shown. The first set is based on the PRD failure being a likely scenario. The second set is based on the remaining failure modes examined. For each effect distance the rationale for it is also shown in the table.

Table 16: Effect Distances for Various Targets

Target	Distance (m)		Rationale	
	PRD	No PRD	PRD	No PRD
Structures	19	11	2 psi overpressure, PRD failure	2 psi overpressure, internal leak
Exposed persons	37	14	0.4 psi overpressure, PRD failure	Flash burn, regulator failure
High flammability materials	16	14	Flash burn distance, PRD failure	Flash burn distance, regulator failure
Low flammability materials	11	9	9.5 kW/m ² steady burn, PRD failure	Cloud extent, ground level 150 psig
Hazardous material storage	9	9	Cloud extent, ground level 150 psig	Cloud extent, ground level 150 psig
Windows, HVAC intakes, etc. below 3 m	19	11	2 psi overpressure, PRD failure	2 psi overpressure, internal leak
Windows, HVAC intakes, etc. above 3 m	28	26	Cloud extent above 3 m, PRD failure	Cloud extent above 3 m, regulator failure
Ignition sources	9	9	Cloud extent, ground level 150 psig	Cloud extent, ground level 150 psig

The basic rationale for the effect distances above is as follows. For structures the distance is based upon the potential detonation of the hydrogen cloud which could result in structural damage. These distances were longer than those resulting from high heat fluxes due to quasi-steady burning of the release. Wall openings and HVAC inlets are based upon the larger of the

structural failure distance or the cloud extent at the elevation of opening or intake. Hazardous material effect distances are based upon the jet extent at ground level which could result in flame impingement for an extended period of time. The effect distances for high flammability materials were based upon the flash burn distance which could result in ignition of these materials. The effect distances for low flammability materials were based upon the longer of the harm effect radiative flux or the jet extent at ground level. Ignition sources had their distance based upon the assumption of a near ground source and the jet extent at ground level. Places where people would assemble or otherwise be present in the open had distances based on the larger of the glass breakage overpressure or flash burns.

It is noted when the PRD failure is not considered, that many of the effect distances are being driven by the regulator failure scenario. It was observed in Section 2.2 that the regulator flow rate provided as an initial condition seemed to be quite high. If the regulator flow rate was a factor of 5 or 10 lower, then the internal piping scenario would dominate and most distances could be reduced by a large amount.

The distances in the current study are all larger, and in most cases substantially so, as compared to the current NFPA 55 requirements. However, this study only examined the potential outcome of a hydrogen release and the combined likelihood of a release in conjunction with an ignition source was not accounted for. A full assessment of the risk would likely result in smaller separation distances.

9.0 ACKNOWLEDGEMENTS

The author thanks the Fire Protection Research Foundation for providing the funding for this study. Along with the support from the Fire Protection Research Foundation, the author thanks the members of the Project Technical Panel for their time and guidance.

